ACKNOWLEDGEMENT

Thanks to Secretaría Nacional de Educación Superior, Ciencia y Tecnología (SENESCYT) for giving me the opportunity to continue my studies at the Universitat Politècnica de Catalunya.

I express my sincere thanks to Professor José Luis Cortina for giving me the opportunity to integrate his research team during the development of Master's final project, for his professionalism, availability and generosity throughout the process.

Special thanks to the many individuals who helped me through my stay in Barcelona. Also to my laboratory colleagues for their support, patience and friendship.

Thanks to my family and all who have crossed in my way for good luck or bad luck and made me smile.

ABSTRACT

The purification of chlorine from brines using polymeric hydrophobic membranes has been evaluated in this work. The objectives have been both to determine the suitable membrane to efficiently transport chlorine and the best operational conditions. Fluoride based polymeric membranes like Polytetrafluoroethylene (FGLP) and (Polyvinylidene fluoride (GVHP) have been selected. Mass transport properties of these membranes have been determined experimentally using flat-sheet membrane modules. The transported chlorine is stabilized in the receiving phase using concentrated solutions of NaOH. The experimental studies have been carried out with under different initial total chlorine concentration and pH. It was determined that most efficient membrane for purification of chlorine is GVHP as provided higher permeability ($3.11x10^{-3}m.s^{-1}$) values in all operating conditions; the mass transfer coefficient for the membrane varied from $7.59x10^{-7}$ to $5.31x10^{-5}cm.s^{-1}$ while for the FGLP membrane varied from $1.27x10^{-6}$ to $1.90x10^{-5}cm.s^{-1}$. The membranes showed to be resistant to the oxidizing conditions of these solutions as demonstrated by FT-IR and SEM-EDS. Chlorine speciation is affecting the strongly the mass transport properties and for example HOCl species are transported in major proportion when the pH of the feed solutions is higher than 2 than the Cl_2 species. The experimental results demonstrated the strong influence of the membrane permeability to chlorine species on the pH of the feed solution.

Keywords: Liquid-liquid contactor, Polytetrafluoroethylene (FGLP) and Polyvinylidene fluoride (GVHP) membranes, Chlorine purification, permeability.

TABLE OF CONTENTS

1. INTRODUCTION

Water is essential for life, the amount of fresh water on earth is limited, and its quality is under constant pressure. Preserving the quality of fresh water is important for the drinking-water supply, food production and recreational water use. Water quality can be compromised by the presence of infectious agents, toxic chemicals, and radiological hazards (WHO). Safe and clean drinking-water is an essential element of health security and underpins sustainable socio-economic development. Global climate change, a growing global population, water requirements to support food security and rapid urbanization all contribute to increased water scarcity and compound the challenge of providing safe drinking-water. In many parts of the world there is a need to develop and manage alternative sources of safe drinking-water. Advances in membrane technology have made desalination of seawater and brackish waters an increasingly viable alternative to produce safe drinking-water (World Health Organization, 2001).

Although there are a number of studies on the use of gas-liquid membrane contactors for gas absorption and stripping, there are only few studies reporter on the use of liquid-liquid membranes contactors to recover ammonia from aqueous solutions (Hasanoglu, 2010; Zhu, 2005 and Norddahl, 2006).

Hollow fiber membranes allowed to predetermin substances to pass through the hollow fiber membrane. Then by, selection of the suitable membrane it is possible to separate target molecules from complex mixtures. In this work hydrophobic membranes of Polytetrafluoroethylene (PTFE) Polyvinylidene fluoride (PVDF) in order to transport chlorine species from brine solutions to sodium chloride solutions as receiving phase were used. The hydrophilic hollow fiber membrane separates two phases; the feed phase containing with the chlorine species ($Cl_{2(g)}$/HClO/ClO^-) and the second phase or receiving solution containing a diluted solution of sodium hydroxide (5%) An air gas gap fills the pores of the hydrophobic membrane, which is not wetted by both aqueous solutions. First chlorine species($Cl_{2(g)}$ or

$HClO_{(g)}$) diffuses from the bulk of the feed to the feed-membrane interface, the Cl_2 / $HClO_{(g)}$ volatilizes through the feed membrane interface, diffuses across the air-filled pore of the membrane, and finally reacts immediately with sodium hydroxide on the interface to form nonvolatile compound (ClO^-).

2. OBJECTIVES

Purification of chlorine from brines using membranes is a field that has study need, which makes innovative work; this is a system liquid-gas-liquid.

Purification of chlorine from brines using hydrophobic polymeric membranes has been postulated as a new solution to prepare highly pure chlorine solutions to be used in water potabilization.

The objectives set for this work are:

- Identifying suitable membrane for the transport and separation of chlorine from brine.

- Identify the operational conditions for acquiring the highest quality of hypochlorite produced.

- Identify the physical-chemical processes employed in the transport of chlorine in hydrophobic membranes.

3. LITERATURE REVIEW

3.1. INDUSTRIAL TECHNOLOGIES FOR CHLORINE PRODUCTION

Chlorine is produced by passing an electric current through a solution of brine (common salt dissolved in water). This process is called electrolysis.
The production of chlorine is performed by means of three existing technologies, according to the cell type used:

- Membrane cell.
- Mercury cells.
- Diaphragm cells.

The stages of the process of obtaining chlorine used in all three technologies are:

- Purification of the brine formed by dissolving sodium chloride or deposits from natural deposits, or directly taken from the sea.
- Electrolysis of NaCl solutions.
- Purification of the products obtained.

The purification step of the brine is necessary since the dissolution of sodium chloride is not pure alkaline earth metal-containing precipitate in the electrolysis, decreasing the current efficiency and life of the electrodes, diaphragms and membranes.

3.1.1. The membrane cell process

The two electric connection points of each chlorine production cell, the anode and the cathode, are separated by an ion-exchange membrane. Only sodium ions and a little water pass through the membrane.
The brine is de-chlorinated and re-circulated. Solid salt is usually needed to re-saturate the brine. After purification by precipitation-filtration, the brine is further purified with an ion exchanger.

The caustic solution leaves the cell with about 30% concentration and, at a later stage in the process, is usually concentrated to 50%. The chlorine gas contains some oxygen and must often be purified by liquefaction and evaporation.

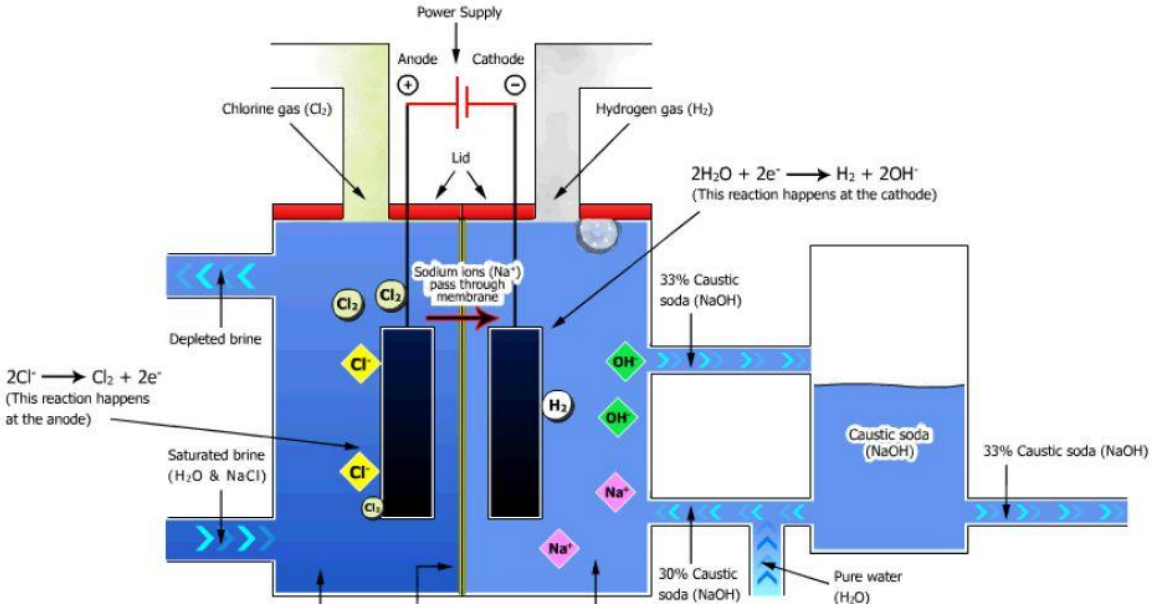

Figure 3.1. Electrolytic membrane cell (EuroChlor, 2011)

The consumption of electric energy is the lowest of the three processes and the amount of steam needed for concentration of the caustic is relatively small (less than one tonne per tonne of caustic soda).

Chlorine producers across Europe are progressively moving towards this method of making their product as the membrane cell process is the most environmentally way of manufacturing chlorine. In 2010, membrane cell capacity accounted for 51.2% of total installed chlorine production capacity in Europe.

3.1.2. The mercury cell process

In the mercury cell process, sodium forms an amalgam with the mercury at the cathode. The amalgam reacts with the water in a separate reactor (decomposer) where hydrogen gas and caustic soda solution at 50% are produced.

As the brine is usually re-circulated, solid salt is required to maintain the saturation of the salt water. The brine is first de-chlorinated and then purified by a precipitation-filtration process. The products are extremely pure. The chlorine, along with a little oxygen, generally can be used without further purification.

This technology will be left to be used on the next years will be replaced by new technologies such as membranes.

3.1.3. The diaphragm cell process

Diaphragm -processIn the diaphragm cell process the anode area is separated from the cathode area by a permeable diaphragm. The brine is introduced into the anode compartment and flows through the diaphragm into the cathode compartment.

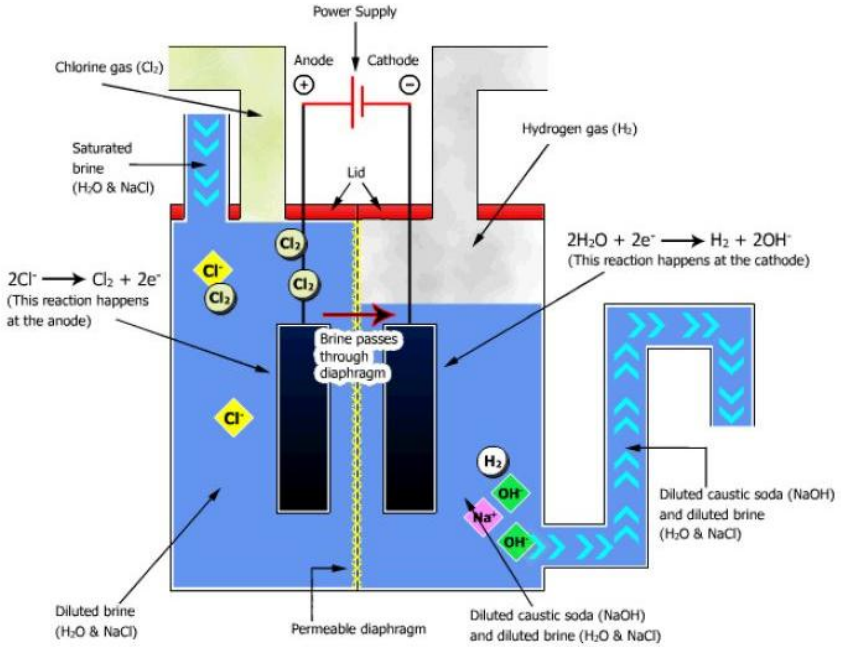

Figure 3.2. The diaphragm cell process

Diluted caustic brine leaves the cell. On various sites, evaporation of caustic is not needed because of a site-specific process integration, technology and management of the energy balance. The caustic soda can also be concentrated to 50% and the salt removed. This is often by using an evaporative process with about three tonnes of steam per tonne of caustic soda.

The salt separated from the caustic brine can be used to saturate diluted brine. The chlorine contains oxygen and must often be purified by liquefaction and evaporation.

In 2010, the diaphragm process accounted for nearly 14% of total installed European chlorine production capacity.

3.1.4. Comparison of cell technologies

Table 3.1 compares the process conditions for the three technologies currently in use (Bommaraju, et al., 2007).

Condition	Mercury	Diaphragm	Membrane
Operating current density(kA/m^2)	8-1.3	0.9 -2.6	03-5
Cell Voltage	3.9-4.2	2.9-3.5	3-3.6
NaOH strength (wt%)	50	12	33-35
Energy consumption (kWh/MT Cl_2)	3360 (10)	2720 (1.7)	2650 (5)
Steam consumption (kWh/MTCl_2)for concentration to 50% NaOH	0	610	180

Table 3.1 Process conditions of the electrolytic cells

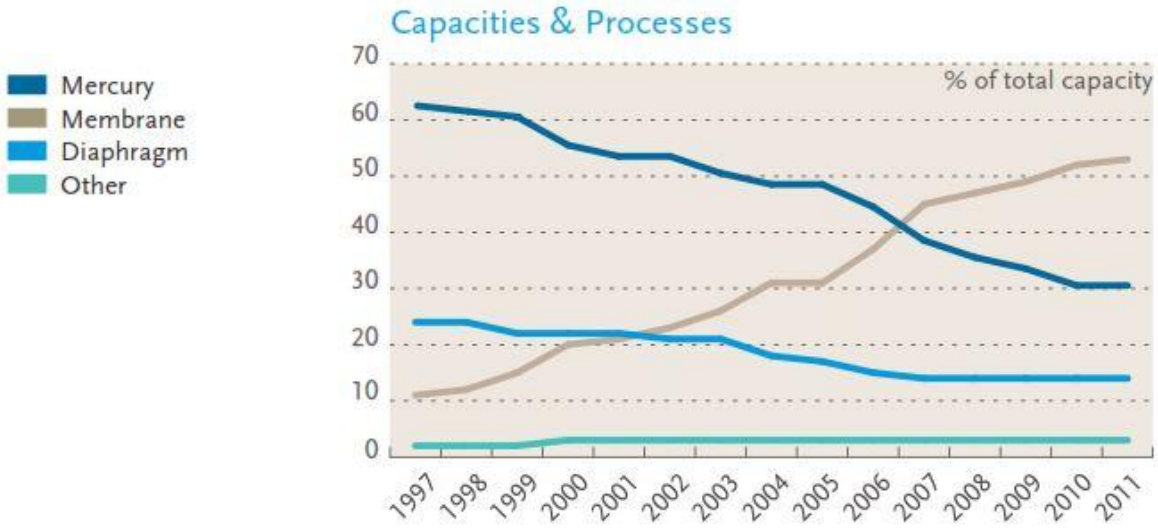

Figure 3.3. Production of electrolytic cells (EuroChor, 2011)

Figure 1.3 shows the production capacity of chlorine using electrolytic cells, and as the mercury cell is declining due to European Union legislation which prohibits industries from

producing chlorine using the process from 2020. This has allowed the use of membranes as an emerging technology (Eurochlor, 2011).

3.2. ON-SITE TECHNOLOGIES FOR PRODUCTION OF CHLORINE: ECTROCHLORINATION

The electrochlorination process is a recognized method of on-site producing low strength liquid chlorine (Sodium Hypochlorite) by on-site electrolysis. The basic components are salt, water or brine and electrical power.

Over recent years electrochlorination has gained favour as a safe, reliable and economic method of disinfection. It is well suited to the treatment of drinking water, wastewater, cooling systems and swimming pools. While the capital cost may be a consideration, the significantly lower operating cost and high level of safety means Electrochlorination is appropriate in many instances.

3.2.1. Electrochlorination Technology

Electrochlorinators are used for the electrolysis of sodium chlorine brine to produce sodium hypochlorite in-situ. The overall reaction process is presented in Equation (3.1). This process can take place mainly in two types of cells: in single cells or cell membranes, it cans be continuously (with a continuous flow) or in a discontinuous (batch).

$$\mathrm{NaCl} + \mathrm{H_2O} + \mathrm{electricity} \rightarrow \mathrm{H_2} + \mathrm{NaOCl} \qquad \text{Eq. (3.1)}$$

The cells consist of a single watertight with two electrodes which apply a potential difference on the brine, as shown in Figure (3.4) Because there is no separation between the products obtained by electrolysis (chlorine and caustic soda), sodium hypochlorite is produced directly and hydrogen, according Equation (3.1). This hypochlorite produced tends to have lower concentrations than that obtained in the cell membrane and has poorer quality, to introduce higher concentrations of NaCl.

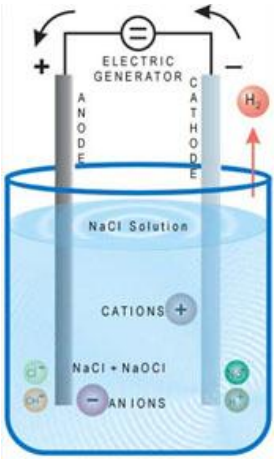

Figure 3.4. Schematic of an electroclorador

In the cell membrane process, the solution of the anode compartment and cathode compartment solution are separated by a cation exchange membrane that selectively allows the passage of sodium ions and prevents the migration of hydroxyl ions from the cathode solution to the anodic, as shown in Figure (3.5) This flow produces a cathode of a solution of caustic soda (NaOH) containing a low concentration of sodium chloride. The main advantages of membrane process are its high energy efficiency and the ability to produce, without adverse environmental effects, a highly concentrated solution of caustic soda high purity and, besides, high concentrations of NaOCl when mixing the products obtained.

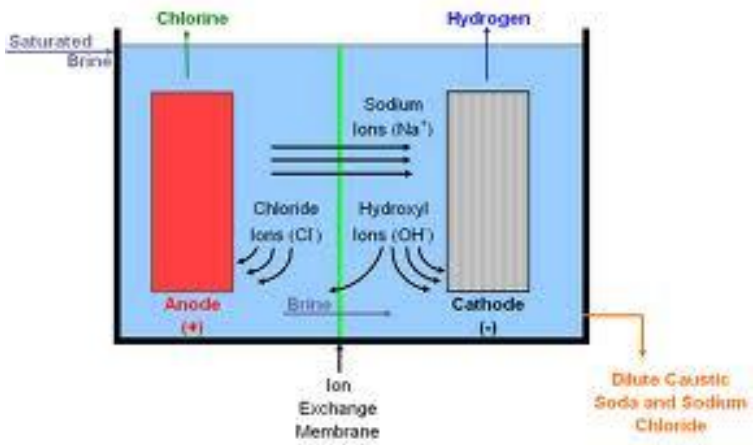

Figure 3.5. Scheme of a membrane electrolysis cell

Reaction at the Electrochlorinators Anode:

$$2Cl \rightarrow Cl_2 + 2e^- \text{ (chlorine generation in the electrolyzer)} \qquad \text{Eq. (3.2)}$$

Reaction at the Electrochlorinator Cathode:

$$2H_2O + 2e^- \rightarrow H_2 + 2OH^- \text{ (hydrogen evolution from electrochlorinator)} \quad \text{Eq. (3.3)}$$

Chemical Reaction in Electrolyzer:

$$Cl_2 + 2OH^- \rightarrow Cl^- + ClO + H_2O \quad \text{Eq. (3.4)}$$

$$NaCl + H_2O = NaOCl + H_2 \text{ (hypochlorite or hypo generation)} \quad \text{Eq. (3.5)}$$

3.3. REACTIVITY OF CHLORINE WITH INORGANIC AND ORGANIC SPECIES IN WATER

Due to their capability for disinfection (e.g. microorganisms) and oxidation (e.g. taste and odor control, elimination of micropollutants, etc.), chemical oxidants (i.e. ozone, chlorine, chlorine dioxide, chloramines, etc.) are commonly used in water treatment processes (Debore and von Guten, U, 2008)

Owing to its low cost, chlorine is globally the most used chemical oxidant for drinking water disinfection. Drinking water disinfection commonly involves the use of chlorine at one or two point(s) in the treatment process, i.e., for pre-treatment (to induce a primary disinfection at the beginning of the treatment process) and/or for post-treatment (to maintain a disinfectant residual in the distribution system). Despite its low activity on microorganisms in biofilms, chlorine can lead to a significant removal of the majority of planktonic bacteria.

Similar to other disinfection processes, chlorination presents certain disadvantages in spite of its broad use and its benefits for the improvement of microbial water quality:

(i) Due to its pH-dependent aqueous chemistry, various species of chlorine (HOCl, ClO^-, Cl_2, etc.) may be present in solution. These forms of chlorine show significant differences in their reactivity with microorganisms and micropollutants. Therefore, variability in oxidation or disinfection efficiency can be observed depending on the pH of the water. (ii) Chlorine interacts with dissolved natural organic matter (DNOM). Numerous so-called disinfection by-products (DBPs) can result from the reaction of chlorine with DNOM. Among these DBPs, trihalomethanes (THMs) and haloacetic acids (HAAs) were the first chlorine DBPs reported

and are currently regulated in the EU (THMs) and the USA (THMs, HAAs). Currently, about 600 DBPs are identified, among them some highly toxic compounds such iodine and bromine iodine and bromine compounds (Bichsel and von Gunten, 2000; Richardson et al., 2003). (iii) Because organic micropollutants are typically not mineralized, numerous transformation products can be formed as a result of the oxidation of organic compounds during water chlorination processes. Little is known on the stability and the biological effects of these compounds. However, in some cases, certain transformation products are fairly stable against further transformation and could persist for hours to days even in presence of residual chlorine. (iv) In bromide-containing waters, chlorination leads to bromine formation. Bromine is usually more reactive than chlorine, especially with phenolic compounds. Under these conditions, bromination can be highly significant and brominated products can be formed (Gallard et al., 2003).

3.3.1. Aqueous chlorine chemistry

In water treatment, gaseous chlorine Cl_2 or hypochlorite are commonly used for chlorination processes. Chlorine gas (Cl_2) hydrolyzes in water according to the following reaction:

$$Cl_2 + H_2O \underset{k_{-1}}{\overset{k_1}{\rightleftharpoons}} HOCl + Cl^- + H^+, K_{Cl_2=k_1/k_{-1}} \qquad \text{Eq. (3.6)}$$

Where k1 and k-1 values, calculated at μ= 0 M and 25 °C from Wang and Margerum, are 22.3s^{-1} and 4.3 x10$^4M^{-2}s^{-1}$, respectively. For temperatures between 0 and 25 °C, K_{Cl2} ranges from 1.3x10$^{-4}M^2$.Hypochlorous acid resulting from reaction Equation (3.6), is a weak acid which dissociates in aqueous solution:

$$HOCl \rightleftharpoons ClO^- + H^+, K_{HOCl} \qquad \text{Eq. (3.7)}$$

with K_{HOCl} reported in literature between 1.5 x10^{-8} ($pK_{HOCl,0\,°C}$=7.82) for temperatures between 0 and 25 °C. Under typical water treatment conditions in the pH range 6–9, hypochlorous acid and hypochlorite are the main chlorine species. Depending on the temperature and pH level, different distributions of aqueous chlorine species are observed. Figure (3.6) shows the distribution of Cl_2, HOCl and ClO^- as a function of the pH at 25 1C and for a chloride concentration of 5 x10^{-3}M (177.5 mg.L^{-1}). For these high chloride concentrations, Figure (3.6) shows that Cl_2 hydrolysis is almost complete at pH>4. Therefore, Cl_2 can usually be neglected under typical drinking water treatment conditions.

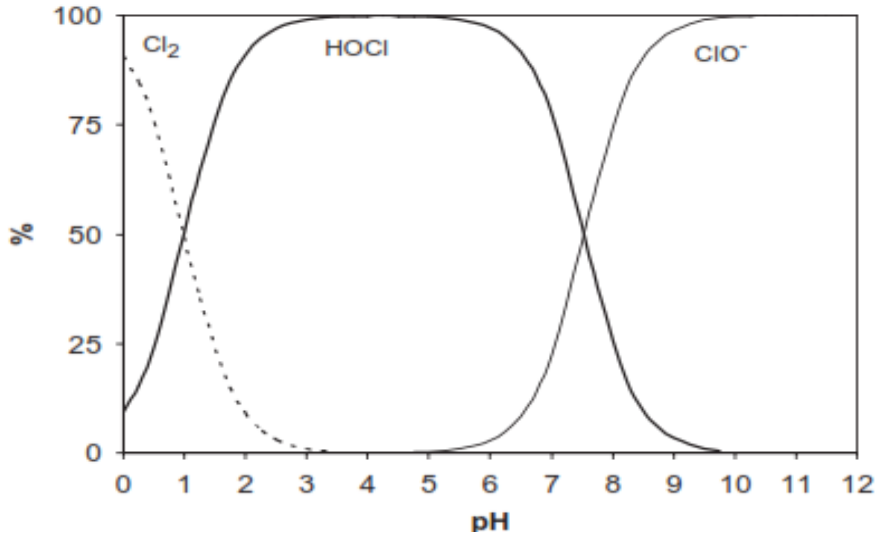

Figure 3.6. Relative distribution of main aqueous chlorine species as a function pH at 25°C and for a chloride concentration of 5 x10^{-3}M (177.5 mgL^{-1})

In addition to these major chlorine species, other chlorine intermediates, including trichloride (Cl^{-3}) and chlorine hemioxide (Cl_2O) or $H2OCl^+$ species, mainly induced at pH <4 and recently discussed can also be formed figure (3.7). In solution, ratios of these compounds are a function of temperature, pH and chloride concentration. Under typical water treatment conditions, their concentrations are very low.

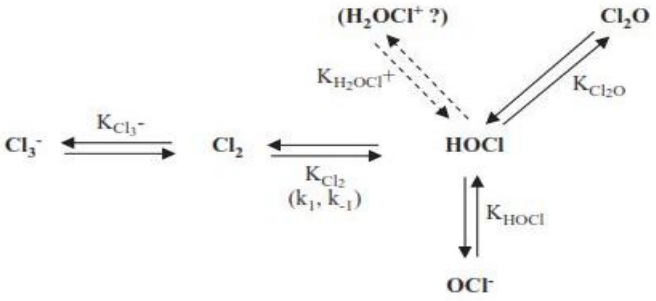

Equations	equilibrium constants (25°C)	references
$HOCl \rightleftarrows ClO^- + H^+$	$K_{HOCl} = 2.9 \times 10^{-8}$	Debordea and von Gunten, 2008
$Cl_2 + H_2O \rightleftarrows HOCl + H^+ + Cl^-$	$K_{Cl_2} = 5.1 \times 10^{-4}\ M^2$ ($k_1 = 22.3\ s^{-1}$, $k_{-1} = 4.3 \times 10^4\ M^{-2}\ s^{-1}$)	
$H_2OCl^+ \rightleftarrows HOCl + H^+$	$K_{H_2OCl^+} = 10^{-3}$-10^{-4}	
$2\ HOCl \rightleftarrows Cl_2O + H_2O$	$K_{Cl_2O} = 8.7 \times 10^{-3}$	
$Cl_2 + Cl^- \rightleftarrows Cl_3^-$	$K_{Cl_3^-} = 0.191$	

Figure 3.7. Chlorine equilibria in solution at 25 °C.

3.3.2. Oxidation of inorganic compounds

Due to its acid–base character, two species of ammonia (NH_3 and NH_4^+) are present in aqueous solutions. Chlorine NH_4^+ species was reported to be negligible. During aqueous chlorination, hypochlorous acid reacts with NH_3 to generate NO_3^- and N_2 for [HOCl]»[NH_3]. This oxidation results from successive reactions which firstly induce chloramine (mono-, di- and trichloramines) formation Equations (3.8)–(3.10)

$$NH_3 + HOCl \rightarrow NH_2Cl + H_2O, \quad \text{Eq. (3.8)}$$

$$NH_2Cl + HOCl \rightarrow NHCl_2 + H_2O, \quad \text{Eq. (3.9)}$$

$$NH_3 + HOCl \rightarrow NCl_3 + H_2O, \quad \text{Eq. (3.10)}$$

Table 3.2 reports rate constants for Equations (3.8) – (3.9) at 25°C and illustrate the temperature dependence of these rate constants. These results show that the chlorine reactivity decreases as the number of chlorine atoms on the nitrogen increases. This is a confirmation of the presumed initial mechanism of an electrophilic attack of HOCl on the chloramine nitrogen. Concerning Equation (3.10), a general-base-catalyzed mechanism was proposed with more complex reaction kinetics. Therefore, no rate constant for chlorine reaction with $NHCl_2$ was reported in Table 3.2. As previously suggested for Equations (3.8) and (3.9), an electrophilic attack of hypochlorous acid on the dichloramine nitrogen was hypothesized for trichloramine formation. In the latter case, this electrophilic attack would be accompanied by a simultaneous general-base-assisted removal of a proton from dichloramine.

3.3.3. Halides and other anionic inorganic compounds

During chlorination, due to chlorine and halide standard redox potentials, hypochlorous acid and hypochlorite can oxidize bromide and iodide. Rate constants for these reactions are summarized in Table 3.2. Due to its high oxidizing capability, hypochlorous acid is the dominant reactive species for the reaction with halides ($k_{HOCl} \geq X10^6\ k_{ClO^-}$).

A mechanism via Cl^+ transfer from hypochlorous acid to the halide (X^-) was proposed for these compounds. This mechanism results in an XCl-type intermediate which then mainly leads to OX^- due to hydrolysis.

$$HOCl + X^- \rightarrow XCl + OH^-, \qquad \text{Eq. (3.11)}$$

$$XCl + 2OH^- \rightarrow OX^- + Cl^- + H_2O \qquad \text{Eq. (3.12)}$$

As shown earlier in the case of chloride in acidic solution, a HOCl acid-catalyzed reaction was also described in the case of bromide and iodide Equation (3.13).

$$HOCl + H^+ + X^- \rightleftharpoons H_2O + XCL \qquad \text{Eq. (3.13)}$$

Table 3.2. Kinetics of oxidation of selected inorganic compounds with chlorine

Compounds	N[a]	pK_a	Elementary reaction rate constants (25 °C)			Apparent rate constants at given pH or pH 7[b] (25 °C)	Arrhenius equation (with K_{HOCl} in $M^{-1}s^{-1}$ and T, temperature in Kelvin)	References
			k_{HOCl+H^+} ($M^{-2}s^{-1}$)	k_{HOCl} ($M^{-1}s^{-1}$)	k_{ClO^-} ($M^{-1}s^{-1}$)	k_{app} ($M^{-1}s^{-1}$)		
Ammonia (NH_3)		9.25		3.07×10^6		1.3×10^{6b}	$k_{HOCl} = 5.4 \times 10^9 \exp(-2237/T)$	
				4.2×10^6		1.8×10^{6b}	$k_{HOCl} = 6.6 \times 10^8 \exp(-1510/T)$	
				2.9×10^6		1.3×10^{6b}		
Chloride (Cl^-)	3.04		2.8×10^4					Debordea and von Gunten, 2008
Bromide (Br^-)	3.89			6.84×10^3		5.3×10^{3b}	$k_{HOCl} = 1.57 \times 10^8 \exp(-1620/T)$	
				2.95×10^3		2.3×10^{3b}		
			1.32×10^6	1.55×10^3				
					9×10^{-4}	1.2×10^{3b}		
Iodide (I)	5.04		3.5×10^{11}	1.4×10^8		1.1×10^{8b}		
					<30			

[a] Nucleophilicity, obtained from Hine (1962).
[b] Calculated from literature data for pH 7 (by considering $pK_{HOCl} = 7.54$ and pK_a compound values reported in the table).

As shown in the case of non-acid-catalyzed reactions, rate constants of HOCl acid-catalyzed reactions with halides increase in the order $Cl^- < Br^- \leq I^-$ (Table 3.2). This order of reaction rates is in agreement with the nucleophilic character (represented by N and reported in Table 3.2) of each of these ions (Hine, 1962). It confirms the initial electrophilic mechanism suggested for these anions.

As a result of oxidation of bromide- and iodide-containing waters, bromine and iodine can be formed during chlorination. Similar to chlorine, these entities have electrophilic properties

which can lead tobrominated and iodinated products. Similar to halides, the oxidation of SO_3^{2-}, CN^-, NO_2^-, mainly occurs via the HOCl species. HOCl reacts with an initial electrophilic attack via Cl^+ which leads to$ClSO_3^-$, ClCN, $ClNO_2$. After hydrolysis, $ClSO_3^-$ and ClCN yield SO_4^{2-} and OCN^-, respectively, whereas $ClNO_2$ results in NO_3^- formation. Two reaction pathways for $ClNO_2$ decomposition to NO_3^- can occur: Either loss of Cl^- to yield NO_2^+, then NO_3^- Equations (3.14)-(3.15), or reactions with NO_2^- to firstly induce N_2O_4 and then NO_3^- Equations (1.16) and (1.17).

$$N_2Cl \rightleftharpoons NO_2^+ + Cl^-, \qquad \text{Eq. (3.14)}$$

$$NO_2 + OH^- \rightarrow NO_3^- + H^+, \qquad \text{Eq. (3.15)}$$

And/or

$$NO_2Cl + NO_2^- \rightleftharpoons N_2O_4 + Cl^-, \qquad \text{Eq. (3.16)}$$

$$N_2O_4 + OH^- \rightleftharpoons N_2O_4 + NO_3^- + NO_2^- + H^+, \qquad \text{Eq. (3.17)}$$

Because in the case of NO_2^- the initial step is reversible Equation (3.11) and followed by two parallel reaction pathways Equations (1.14)–(1.17), complex chlorination oxidation by HOCl (Lahoutifard et al., 2003)

3.4. PRODUCTION OF HYPOCHLORITE FROM SEAWATER AND SEAWATER DESALINATION: LIMITATIONS OF USE FOR DRINKING WATER

3.4.1. Overview

This European Drinking Water Directive specifies requirements for minimum purity of sodium hypochlorite used for the treatment of water intended for human consumption. They have established limits for impurities commonly present in this product. The product must meet the requirements specified in Table 3.1.

Table 3.3. Chemical Parameters for hypochlorite from seawater and seawater desalination limits

Parameter		**Limit in mg / kg of chlorine available**	
		Type 1	**Type 2**
Arsenic (As)	max.	1	5
Antimony (Sb)	max.	20	25
Cadmium (Cd)	max.	2.5	5
Chromium (Cr)	max.	2.5	5
Lead (Pb)	max.	15	15
Mercury (Hg)	max.	3.5	5
Nickel (Ni)	max.	2.5	10
Selenium (Se)	max.	20	25
Selenio (Se)	max.		
		Limit in g/kg of Chlorine available	
Sodium bromate[a]	max.	2.5	5
NOTE cyanide cannot exist in half as strong oxidizing sodium hypochlorite and, therefore, is not relevant as chemical parameter. Pesticides and polycyclic aromatic hydrocarbons are byproducts of the manufacturing process. In connection with the parametric values of sodium hypochlorite for the content of traces metals in drinking water [Directiva 98/83/CE].			
[a] Sodium bromate is a subproduct of the manufacturing process.			

3.5. PROCESSES AND MECHANISMS OF FORMATION OF BROMATES

Sodium and potassium bromate are powerful oxidizers used mainly in permanent wave neutralizing solutions and the dyeing of textiles using sulfur dyes. Potassium bromate has also been used as an oxidizer to mature flour during milling, in treating barley in beer making and in fish paste products, although the Joint FAO/WHO Expert Committee on Food Additives (JECFA) has concluded that the use of potassium bromate in food processing is not appropriate. Bromate is not normally found in water, but can occur as a result of pollution from industrial sources, sometimes as a consequence of its presence in contaminated soil. However, the main source in drinking-water is its formation during

ozonation when the bromide ion is present in water. Bromate may also be formed in hypochlorite solutions produced by electrolysis of bromide-containing salt.

Bromate is difficult to remove once formed. By appropriate control of disinfection conditions, it is possible to achieve bromate concentrations below 0.01 mg/litre (WHO, 2003).
The objective is to produce a hypochlorite solution free of bromates (BrO_3^-)

3.6. PURIFICATION PROCESSES $CL2_{(g)}$ BASED ON LIQUID-LIQUID CONTACTORS

3.6.1. Basis and principles of gas transport in membranes

The chlorine gas coming from the electrolysis in the current process is concentrated in Cl_2 (90-95%), the rest being air leaking into the system. The oxygen has to be removed before H_2 is reacted with Cl_2 further down the line in order to avoid the formation of water.

3.6.2. Membrane types

The diversity of membrane based separation systems makes it difficult to categorize them clearly. The systems are typically labeled either on the basis of type of membrane employed, or on the driving force applied to assist penetrant transport through the membrane (Bitter, 1991). The type of membranes used for separation are classified as porous, non-porous (tight) and liquid membranes.

Porous Membranes

Porous membranes are studied in terms of their pore size. These are then classified as either microporous or ultraporous membranes. The microporous membranes have pore sizes in the range of 200 to 3000 nm, with the transport of penetrant molecules through these pores labeled as viscous (Poiseuille) type (Bitter, 1991; Eykamp,1995). The pressure driven molecules then low through the membrane independent of their size, shape or mass, thereby rendering the microfiltration process as nonselective on a molecular scale.

The micropores membranes, with a pore size of less than 10 nm, are more useful for penetrant separation on a molecular level. The separation is mainly achieved by "sieving" of the molecules. Although, steric hindrance at the entrance of the pores and frictional resistance in the pores also play an important role during the separation process. The penetrant transport is labeled as "Knudsen Flow", where the pore size of the membrane is smaller than the mean free path of the molecules. The diffusion rate of the molecule is then related to the inverse square root of its molar mass (Baker, 1991; Eykamp, 1995). The separation achieved is very low, except for the case where molecules with significant molecular weight difference are being separated.

Liquid Membranes

A liquid membrane is a stable emulsion of an aqueous reagent solution and an immiscible hydrocarbon phase and is primarily used in the separation of liquids. The liquid membrane solution physically separates the feed solution from the permeate solution, as both solutions are immiscible in the liquid membrane (Bitter, 1991). With favorable thermodynamic conditions being maintained at the two interfaces, the solute is transferred from the feed to the permeate solution. A complexing agent is sometimes added to the liquid membrane to expedite the solute transfer. This assisted process is then accordingly named as "facilitated transport" or mediated transport (Boyadzhiev and Lazarova, 1995).

In some cases microporous polymer membranes are impregnated with the liquid membrane solution to provide support and stability. The shortcomings of these supported membranes are observed in loss of liquid to the contacting solutions; low permeate flux, and its high sensitivity to overpressure. The commercial potential for liquid membranes is still in its exploration stage.

Non-Porous Membranes

Non-porous membranes primarily consist of polymer membranes. The non-porous structure of the polymer is related to the non-continuous passages present in the polymer chain matrix. These passages are created and destroyed due to thermally induced motion of the chains. Therefore, the transport of a penetrant is based on its movement through these passages. The effects of penetrant activity (driving force) and operating conditions then play an important role in governing the gas transport rate and separation property of the membrane.

The first non-porous membrane used for separation purposes was natural rubber (Cen and Lichtentharler, 1995.) With the capability of controlling the chemical structure and properties of synthetic polymers, new possibilities were opened to improve the transport and separation properties of membranes.

3.7. FUNDAMENTALS OF GAS TRANSPORT IN MEMBRANES

In this section a simplified development of the theory of gas transport across a membrane is presented. The diffusion of gas through the membrane can be expressed by Fick's first law (Javaid, 2005):

$$J = -\left(\frac{dC}{dX}\right) \qquad \text{Eq. (3.18)}$$

where J is the flux of the gas through the membrane, D is the diffusion coefficient, and dC/dx is the concentration gradient of the gas across the membrane. At steady state, the flux is a constant. If D is assumed to be constant, Equation (3.18) can be integrated to give:

$$J = D\left(\frac{C_0 - C_l}{l}\right) \qquad \text{Eq. (3.20)}$$

where Co and C are the concentration of the gas on the upstream and downstream ends, respectively, and l is the l thickness of the membrane. At low pressures, Henry's law is often adequate to express the concentration of the gas in the membrane:

$$C = Sp \qquad \text{Eq. (3.21)}$$

where S is the Henry's solubility constant and p is the pressure of the gas. By substituting Equation (3.21) into Equation (3.20) we get:

$$J = DS\frac{(P_0 - P_l)}{l} = \bar{P}\frac{(P_0 - P_l)}{l} \qquad \text{Eq. (3.22)}$$

Where $\bar{P}$ is permeability of the gas and according to Equation (3.22) can be defined as:

$$\bar{P} = DS \qquad \text{Eq. (3.23)}$$

The permeability is therefore a product of the diffusivity and solubility coefficients of the gas species. In real systems, the diffusion coefficient D and the solubility coefficient S may both be function of concentration, so the theoretical analysis becomes more complicated. However, the idea of the permeability being the product of a solubility term and a diffusivity term is quite general.

In gas separation with membranes, selectivity is defined as the ratio of the individual gas permeabilities. Based on single gas permeabilities of species “A” and “B” we may write an ideal selectivity as:

$$\alpha_{A/B} = \frac{\overline{P}_A}{P_B} = \frac{D_A}{D_B}\frac{S_A}{S_B} \qquad \text{Eq. (3.24)}$$

The selectivity can therefore be viewed as a function of differences in both the diffusivity and solubility coefficients of the two gases.

Diffusivity-based gas separation is generally employed for chemically similar species like O_2 and N_2, where separation occurs due to the preferential permeation of the smaller more mobile species. In fact most membrane gas separation systems in operation are diffusivity-based. However, in certain industrial and environmental applications, it is preferable to achieve separation based on solubility differences (Javaid, 2005).

The mechanisms are briefly characterized as follows:

Knudsen diffusion; the square root of the ratio of the molecular weights will give the separation factor (typically here 2 and 4 nm glass without pore modification).

Selective surface diffusion; governed by a selective adsorption of the larger (non-ideal) components on the pore surface. For mixed gas an increase in selectivity may be observed if the adsorbed monolayer covering the internal pore walls restricts the free pore entrance so that smaller non-adsorbed molecules cannot pass through (glass with surface modification).

Molecular sieving; the smallest molecules will permeate, the larger being retained (glass and carbon fibre)-(Lindbråthen, Hägg, 2005).

3.8. LIQUID-LIQUID MEMBRANE CONTACTORS

In recent years, membrane contactors have proved to be useful for removing low-concentration solutes from wastewater and they may prove to be an attractive alternative for the present work. Hollow fiber-membrane contactors, usually in a shell-and-tube configuration, offer many advantages over traditional contact operations. Membrane contactors provide a large and stable interfacial area. Two fluids flowing across the hollow fibre allow mass transfer to occur between the fluids. The hydrophobic microporous polymeric membrane provides the transfer area and restricts the permeation of water. The transfer takes place at the pore opening, inside the pore, or at the pore exit. For gases in water, polypropylene (PP), polytetrafluoroethylene (PTFE), and polyvinylidene fluoride (PVDF) are normally used as hydrophobic polymers (Mandowara, 2011).

Several researchers have carried out simulation studies of the degasification of water via convective diffusion using membrane contactors (Mandowara and Bhattacharya, 2009; Kieffer et al., 2008; Al-Marzouqi et al., 2008;Lee et al., 2001). Mandowara and Bhattacharya (2009) simulated ammonia removal by a vacuum application on the shell side and obtained concentration profiles. Kieffer et al. (2008) used computational fluid dynamics to numerically study mass transfer in a liquid-liquid-phase membrane contactor, and they observed a clear separation between the reaction and mixing zones. AlMarzouqi et al. (2008) modelled the chemical absorption of CO_2 in MEA solvent using PP membrane contactors; they considered both radial and axial diffusion under the condition of complete wetting. Lee et al. (2001) studied the removal of CO_2 in a hollowfibre membrane contactor using aqueous potassium carbonate; they derived and numerically solved coupled nonlinear partial differential equations and also reported the optimal absorbent flow rate. Keshavarz et al. (2008a) developed and solved a mathematical model for membrane contactors operated under non-wet or partially wetted conditions during the simultaneous absorption of 2 carbon dioxide and hydrogen sulphide in diethanolamine (DEA) solution.

3.8.1. Gas transport in liquid-liquid contactors

Figure 3.8 shows a schematic of membrane contactor operation in the liquid-liquid extraction mode for performing experimental studies. The model equations were developed by considering aqueous chlorine solutions in the lumen side and aqueous sodium hydroxide in the shell side.

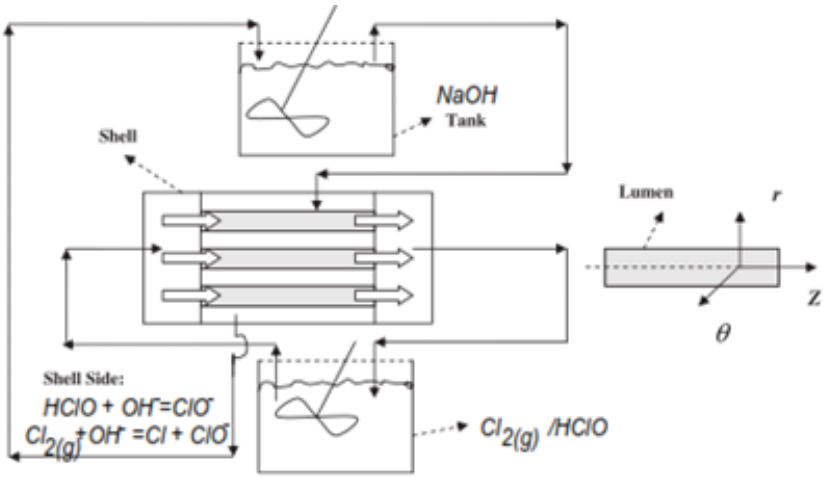

Figure 3.8. . Experimental set-up for membrane contactors operated under liquid-liquid extraction mode for chlorine.

Agitators are used in both tanks to ensure uniform mixing. Both solutions are circulated in loops as shown in Figure 3.8. In the aqueous solution, chlorine exists as both unionized and ionized chlorine. This is an unsteady-state process in which the transport of chlorine and chorine ions is governed by axial diffusion, radial diffusion, and convection in the lumen side. A three-step transport may be considered to occur sequentially during the chlorine removal. The first step is radial diffusion of both ionized and chlorine ions to the internal surface of the hollow fibre. The second step is the diffusion of chlorine inside the pore. Finally, chlorine in gaseous form reaches the interface (located at the pore exit of the hydrophobic membrane) and instantaneously reacts with the extract phase (sodium hydroxide present at the shell side). Because chlorine soluble in sodium hydroxide, no reaction zone is formed; it reacts only at the interface. Given the above considerations, the numerical model is based on the following assumptions:

I. Isothermal operation;
II. Fully developed parabolic profile in the lumen side;
III. No pore blockages and pores are filled with air;

IV. Feed and extract volumes (and hence tank volumes) are large compared to that of the hollow-fibre module;

V. Flow rates of both feed and extract (chorine solution and sodium hydroxide, respectively) are constant because the feed is dilute.

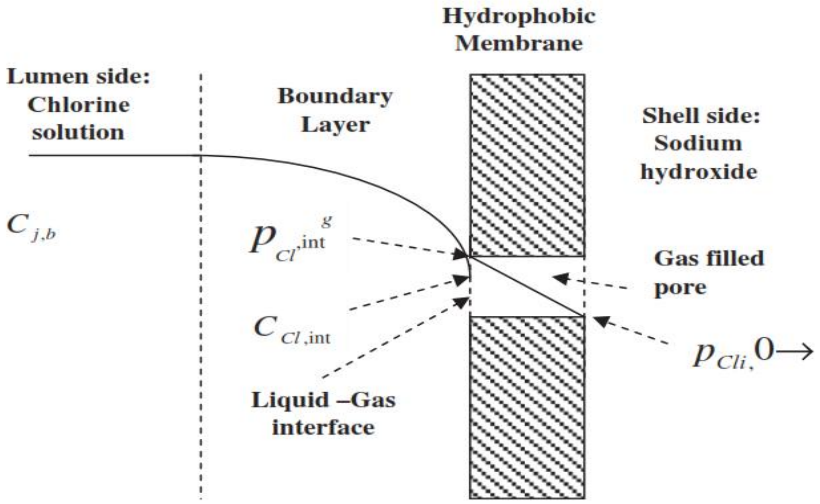

Figure 3.9. Concentration profile for the species j at a particular time when it moves from lumen side towards shell side through a microporous hydrophobic membrane.

Mass balance inside de lumen

The transport of chlorine ions in the lumen is expressed through a convective-diffusive equation (Mandowara and Bhattacharya, 2009):

$$\frac{\partial C_j}{\partial t} + \tilde{U} * \nabla C_j = D_{j\nabla^2 C_j} + R_j \qquad \text{Eq. (3.25)}$$

Where C_j denotes the local combined concentration of chlorine ions (component j), D is the diffusivity of the component in water, R is the rate of generation due to the chemical reaction, and $\tilde{U}$ is the velocity vector. As there is no chemical reaction in the lumen side, symmetry is assumed inside the lumen (cylindrical):

$$\frac{\partial C_j}{\partial \theta} = 0 \qquad \text{Eq. (3.26)}$$

Only diffusion and convection of chlorine are assumed to occur and hence R_j=0. Further, U (the radial velocity), which is due to the diffusion of chlorine in the radial direction, also

becomes zero. This is because the rate of diffusion of chlorine in water is negligible and the bulk flow is in the Z direction (Mandowara and Bhattacharya, 2009). Equation (3.7) can now be written as

$$\frac{\partial C_j}{\partial \theta} U_z \frac{\partial C_j}{\partial Z} = D_J \left\{ \frac{1}{r} \frac{\partial}{\partial r} \left(r \frac{\partial C_j}{\partial r} \right) + \frac{\partial^2 C_j}{\partial Z^2} \right\} \qquad \text{Eq. (3.27)}$$

The velocity distribution in the lumen side under laminar flow conditions can be written (Kreulen et al., 1993) as

$$U_z(r) = 2\left\{1 - \left({}^{r}/_{R}\right)^2\right\} \qquad \text{Eq. (3.28)}$$

Defining Ū to be the average velocity of the fluid inside the lumen:

$$\bar{U} = \frac{Q}{N\pi R^2} \qquad \text{Eq. (3.29)}$$

Boundary conditions

Symmetry inside the fibre: at r =0; all Z and t

$$\left(\frac{\partial C_j}{\partial r}\right)_{r=0} = 0 \qquad \text{Eq. (3.30)}$$

At Z = 0; all r and t

The model is based on an unsteady-state situation considering radial and axial diffusion in the lumen; however, at the entrance, both types of diffusion are neglected. Hence,

$$C_{j,Z} = 0 = C_{tank} \qquad \text{Eq. (3.33)}$$

At Z = L; all r and t

Assuming the diffusion of chlorine at the exit of the lumen (in the Z-direction) to be negligible in comparison to its movement in the same direction due to bulk flow, one may obtain the boundary condition at the exit of the lumen as

$$D_j = \left(\frac{\partial^2 C_j}{\partial Z^2}\right)_{z=L} = 0 \qquad \text{Eq. (3.34)}$$

The above assumption is justified because the bulk movement (convection) of chlorine is more pronounced at the exit of the lumen. Accordingly, at the exit of the lumen, $\partial C_j/\partial_Z$ is a function of *r* only; and hence its variation w.r.t. Z is assumed to be negligible (Treybal, 1981).

At the inner surface of the hollow fibre, the flux of the chlorine aqueous phase equals the flux of the gaseous chlorine diffused through the pore. Therefore, at *r* = R, the boundary condition is described by

$$D_j = \left(\frac{\partial C_j}{\partial r}\right)_{r=R} = k_{g,pore}\left(\frac{P^g_{Cl,int}}{R_g T}\right) \qquad \text{Eq. (3.35)}$$

In this equation, the concentration of chlorine at the pore exit is assumed to be negligible. This is because an instantaneous reaction between basic and chlorine takes place at the pore exit. Further, as described earlier, C_j is the combined concentration of chorine, hypochlorite acid and hypochlorite ions:

$$C_j = C_{Cl_{(g)}} + C_{HClO} + C_{ClO^-} \qquad \text{Eq. (3.36)}$$

At the liquid-gas interface (located at the pore entrance, Figure. 3.2), Henry's law may be applicable:

$$P^g_{Cl,int} = H_{Cl,int} \text{ or } C^g_{Cl,int} = H^*_{Cl,int} \qquad \text{Eq. (3.37)}$$

Further, in the aqueous solution, the following equilibrium is observed:

$$Cl_g + OH^- \overset{k_a}{\leftrightarrow} Cl^- + ClO^- \qquad \text{Eq. (3.38)}$$

$$HClO \overset{k_a}{\leftrightarrow} H^+ + Cl^- \qquad \text{Eq. (3.39)}$$

Where,

$$k_a = \frac{C_{Cl^-} * C_{ClO^-}}{C_{Cl_g} * C_{OH^-}} \qquad \text{Eq. (3.40)}$$

$$k_a = \frac{C_{H^+} * C_{ClO^-}}{C_{HClO}} \qquad \text{Eq. (3.41)}$$

The mass transfer coefficient inside the pore, $k_{Cl.g,pore}$ can be estimated using the following correlation (Mandowara and Bhattacharya, 2009):

$$k_{Cl.g,pore} = D_{Cl,c,pore}\left\{\frac{\varepsilon}{\tau b}\right\} \qquad \text{Eq. (3.42)}$$

where the tortuosity is given by

$$\tau = \frac{1}{\varepsilon^2} \qquad \text{Eq. (3.43)}$$

where,

$k_{Cl,g,pore}$= mass transfer coefficient inside the pore

$D_{(Cl,c,pore)}$= diffusivity in the pore

ε= porosity

τ= tortuosity

Assuming the pores to be sufficiently small, Knudsen and bulk diffusions may co-exist. Thus, the combined diffusivity (Mandowara and Bhattacharya, 2009) $D_{Cl, C, pore}$ is expressed by

$$\frac{1}{D_{Cl,c,pore}} = \frac{1}{D_{k,Cl,pore}} + \frac{1}{D_{Cl,air}} \qquad \text{Eq. (3.44)}$$

Further, the Knudsen diffusion $D_{k,Cl,pore}$ is given by

$$D_{k,Cl,pore} = \frac{d_{pore}}{3}\left(\frac{8R_gT}{\pi M_{Cl}}\right)^{1/2} \qquad \text{Eq. (3.45)}$$

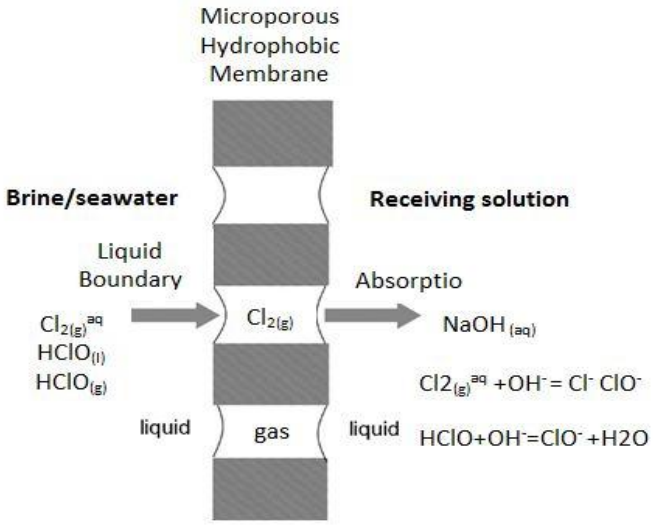

Figure 3.10. Principles of diffusion of chlorine in membrane liquid-liquid

Membrane mass transfer coefficient depends on the pore diameter, porosity to tortuosity ratio and thickness of the membrane. The main aim of any membrane contactor design is to reduce the resistance offered by the membrane (this is the additional resistance developed as compared to any traditional contacting equipment). Larger membrane pore, larger porosity to tortuosity ratio and lesser thickness of the membrane will result in increased mass transfer coefficient of the membrane and hence results in lesser resistance to the mass transfer of chlorine.

4. EXPERIMENTAL METHODOLOGY

4.1. MATERIALS

In present study the permeability of chlorine species were evaluated using fluoride based hydrophobic polymeric membranes, commercially available: of Polytetrafluoroethylene (PTFE) Flouropore FGLP04700 and Polyvinylidene fluoride (PVDF) Durapore GVHP04700 with 0.2um pore size. The description of each membrane is shown in Table 4.1. The experimental module to be used consists of two compartments which are joined by sheet-plain membrane; each compartment has a capacity of 200ml which is equipped with a stirrer and a pH sensor. Brine employed as feed solution was taken from a Reverse Osmosis plant located in El Prat de Llobregat (Barcelona). To decrease the pH of the brine, concentrated hydrochloric acid was used. The receiving phase contained a 5% sodium hydroxide solution.

Table 4.1. Description of membranes used for the chlorine transport experiments

FGLP04700	**GVHP04700**
DESCRIPTION	**DESCRIPTION**
Material: PTFE, hydrophobic	Material: PVDF, hydrophobic
Functional group:-[CF2-CF2]x-	Functional group: -(CH2CF2)x-
Water Flow Rate, mL/min x cm²: 15	Water Flow Rate, mL/min x cm²: 15
Bubble Point at 23 °C: ≥1.0 bar	Bubble Point at 23 °C:≥1.24 bar
Maximum Operating Temperature, °C: 130	-
Filter Type: Screen filter	Filter Type: Screen filter
Pore Size (µm): 0.22	Pore Size (µm): 0.22
Filter Diameter (mm): 47	Filter Diameter (mm): 47
Gravimetric Extractables, %: 0.5	Gravimetric Extractables, %: 0.5
Thickness, µm: 175	Thickness, µm: 175
Air Flow Rate, L/min x cm²: 3	Air Flow Rate, L/min x cm²: 16
Porosity %: 70	Porosity %: 75

Analysis and characterization of virgin and used membrane was carried out by using Fourier Transform Infrared Spectrophotometry (FT-IR) and the Scanning Electron Microscopy and Energy Dispersive X-Ray Spectrometry (SEM-EDS).

Experimental methodoly to study the membrane transport of chlorine and to determine the membrane mass transfer coefficients two main variables were considered: chlorine concentration and pH of the feed solution, Initially the mixing conditions were optimized to reduce the film thickness at the aqueous membrane interfaces resulting in a value of 1200 rpm. The experimental designs of experiments to be performed are summarized in Table 4.2, and overs the expected.conditions of chlorine concentration (150 to 600 ppm) and pH (1 to 7) to be achieved in the electrochlorination of sea water desalination brines. Samples from both aqueous phases (feed and receiving) were taken for analysis of the total chlorine content.

Table 4.2. Operating and sampling for the studies GVHP and FGLP membranes

Membrane	Concentration (ppm)	rpm 1200	Sampling (min)								pH1	pH2	pH4	pH6	pH7
			0	5	10	15	20	30	60	120					
FGLP	150	x	x	x	x	x	x	x	x	x		x		x	
	300	x	x	x	x	x	x	x	x	x	x	x	x	x	x
	600	x	x	x	x	x	x	x	x	x		x		x	
GVHP	150	x	x	x	x	x	x	x	x	x		x		x	
	300	x	x	x	x	x	x	x	x	x	x	x	x	x	x
	600	x	x	x	x	x	x	x	x	x		x		x	

4.2. INSTRUMENTATION AND ANALYTICAL METHODS

4.2.1. Membrane system

The schematic representation of the experimental technique used in this work is shown in Figure 4.1. Module consists of two compartments in batch of 200 mL each one, joined by the membrane under study (Fluoropore FGLP or Durapore® GVHP) (Table 4.1). Each compartment sampling points for the extraction of desired volumes at different time intervals of 0, 5, 10, 15, 30, 60, 90 and 120 minutes. The cell incorporates two sensors for measuring pH and temperature (Crison LPG22 and Crison LPG21+) at each sampling time. A compartment contains brine from electrodialysis, and the other 5% sodium hydroxide solution. The stirrers are adjusted to 1000 rpm for all experiments to achieve the minimum and stable film layers at both aqueous membrane interfaces of both sides. Each

experimental condition was performed at least in duplicate and when required in triplicate when discrepancies in the experimental results were observed..

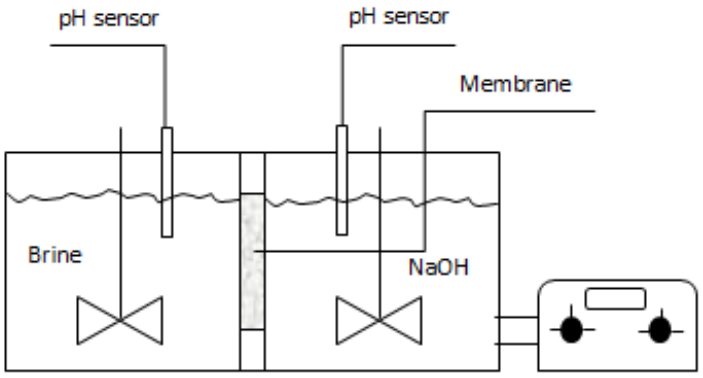

Figure 4.1. Experimental set-up for purification of chlorine produced in electrochlorination by Membrane contactors liquid-liquid

4.2.2. Chlorine analysis

The method used for the determination of chlorine is an iodometric method by manual titration using NaS_2O_3. Calibration curves were made for both the brine as the sodium hydroxide solutions using a correlation coefficient of the calibration curve, equal to 0.9998. The chlorine content is expressed by the following equation:

$$\mathrm{CL_2}\left(\frac{\mathrm{mg}}{\mathrm{Kg}}\right) = \mathrm{Vml} * \frac{0.1\mathrm{meqNa_2SO_3}}{1\mathrm{mlNa_2SO_3}} * \frac{1\mathrm{meqCL_2}}{1\mathrm{meqNa_2SO_3}} * \frac{1\mathrm{mmolCL_2}}{2\mathrm{meqCL_2}} * \frac{71\mathrm{mgCL_2}}{1\mathrm{mmolCL_2}} * \frac{1}{\mathrm{WgBrine}} * \frac{1000\mathrm{g}}{1\mathrm{Kg}} \qquad \text{Eq. (4.1)}$$

4.2.3. Mass balance

Due to the know instability of chlorine solutions a mass balance for chorine species was made, especially at acidic pH values, with the objective to determine the potential losses in the compartments along the experiment lifetime. It was observed they exceed 50% at pH

below 1. This phenomena was present because it was impossible to ensure the total air tightness of the module so the final data analysis requires corrections using the following equations:

Mass balance:

$$CL_{2in} = CL_{2outBrine} + CL_{2out\ NaOH} \quad \text{Eq. (4.2)}$$

Losses:

$$Losses(\%) = 100 - \left(\frac{CL_{2outBrine} + CL_{2out\ NaOH}}{CL_{2in}}\right) * 100 \quad \text{Eq. (4.3)}$$

Where CL represents the number of mols of chlorine species

4.2.4. Determination of membrane permeability

With the diffusion coefficient dependent on gas concentration, the permeation flux is given as:

$$J_i = -\frac{dC_i}{d_t} * \frac{V}{A} \quad \text{Eq. (4.4)}$$

Where

J_i: flux through the membrane

C_i: Concentration

V: Volume of the solution

A: area of passing through the membrane

Flux relationship with the concentration

$$J_i = P_i * C_i \quad \text{Eq. (4.5)}$$

Where

P_i: Permeability

Therefore, from Equations 4.4 and 4.5

$$\frac{dC_i}{d_t} * \frac{V}{A} = P_i * C_i \qquad \text{Eq. (4.6)}$$

Thus the differential equation

$$\int \frac{dC_i}{d_t} = P_i * \frac{A}{V} * \int dt \qquad \text{Eq. (4.7)}$$

Hence,

$$\ln \frac{C}{C_0} = \frac{P_i * A * t}{V} = P_i * C_i \qquad \text{Eq. (4.8)}$$

Then the slope of the function ln (C/C_0) versus t will allow to determinate the membrane permeability by suing the following equation.

$$m = -P_i * \frac{A}{V} \qquad \text{Eq. (4.9}$$

4.2.5. Membrane diffusivity to chlorine species

The membrane diffusivity to chlorine species could be determined, if we take into account the different chlorine species present in solution.

Brine compartment (aqueous phase)

$$HCLO \leftrightarrow OCl^- + H^+ \log Ka \qquad \text{Eq. (4.10)}$$

$$HCLO_{(g)} \leftrightarrow +HCLO_{(aq)} \log K_H \qquad \text{Eq. (4.11)}$$

$$J_{af} = k_{af} * (C_{cf} - C_{cif}) \qquad \text{Eq. (4.12)}$$

$$J_{af} = {k_{af}}^{-1} * \left(\left[HCLO_{(g)} \right]_f - \left[HCLO_{(aq)i} \right]_{if} \right) \qquad \text{Eq. (4.13)}$$

$$\frac{1}{\Delta_{af}} = k_{af} = \frac{D_{af}}{L} \qquad \text{Eq. (4.14)}$$

Where,

J_{af}: Flux in the brine

K_{af}: Mass transfer coefficient in interphase

Δ_{af}= Mass transfer coefficient inverse

D_{af}: Diffusivity membrane

L= Membrane thickness

Membrane pores

$$J_m = k_m = D_{af} = k_{af} * d_a \qquad \text{Eq. (4.15)}$$

$$J_m = k_m * \left([HCLO_{(g)}]_{if} - [HCLO_{(g)Caf}] \right) \qquad \text{Eq. (4.16)}$$

Henry's law may be applicable:

$$J_m = \frac{1}{\Delta m * k_H} * [HCLO_{(g)i}] \qquad \text{Eq. (4.17)}$$

NaOH compartment

$$J_{as} = \frac{1}{\Delta_{NaOH}} * [HCLO_{(g)i}] \qquad \text{Eq. (4.18)}$$

Final equation,

$$J = \frac{[HCLO_{(aq)if}]}{\Delta af + k_H * \Delta m} \qquad \text{Eq. (4.19)}$$

$$J = P * [HCLO_{(aq)}] \qquad \text{Eq. (4.20)}$$

To calculate the mass transfer coefficient is obtained by equalizing the Equations (4.19) and (4.20) considering Equation (4.15), when we assume only one species is present.

$$P = \frac{1}{\Delta_{af} + k_H * \Delta m} \qquad \text{Eq. (4.21)}$$

Consider the species,

$$[HClO]_{TOT} = ([HClO]) + [ClO^-] \qquad \text{Eq. (4.22)}$$

$$J_{af} = \Delta_{af}^{-1} * \left([HClO]_{ToT,f} - [HClO]_{TOT,f}\right) \qquad \text{Eq. (4.23)}$$

$$J_{af}\,\Delta_{af} = \left([HClO]_{ToT,f} - [HClO]_{TOT,f}\right) \qquad \text{Eq. (4.24)}$$

$$J_m = \Delta_m^{-1}\left([HClO]_{g,f} = \Delta_m^{-1} * k_H^{-1}[HClO]_{aq,f}\right) \qquad \text{Eq. (4.25)}$$

$$[HClO]_{aq,f} = J_m * \Delta_m * k_H \qquad \text{Eq. (4.26)}$$

Mass balance of HClO:

$$k_a = \frac{[H^+] * [ClO^-]}{[HClO]_{aq}} \quad \rightarrow \quad [ClO^-] = k_a * [HClO]_{aq} * [H^{+-1}] \qquad \text{Eq. (4.26)}$$

$$[HClO]_{TOT,aq} = [HClO]_{aq} * (1 + k_a * [H^{+-1}]) \qquad \text{Eq. (4.27)}$$

$$J_a\,\Delta_{af} = [HClO]_{aq} * (1 + k_a * [H^{+-1}]) - [HClO]_{aq} \qquad \text{Eq. (4.28)}$$

Where,

$$J_m\,\Delta_m k_H = [HClO]_{aq}$$

$$J_a\,\Delta_{af} = [HClO]_{aq} * (1 + k_a * [H^{+-1}]) - J_m\,\Delta_m k_H \qquad \text{Eq. (4.29)}$$

If,

$$J_{af} = J_m$$

$$J\,(\Delta_a + \Delta_m * k_H) = [HClO]_{aq} * (1 + k_a * [H^{+-1}]) \quad \text{Eq. (4.30)}$$

$$J = \frac{1 + k_a * [H^{+-1}] * [HClO]_{aq}}{(\Delta_a + \Delta_m * k_H)} \quad \text{Eq. (4.31)}$$

$$P = \frac{J}{[HClO]_{aq}} = \frac{1 + k_a * [H^{+-1}]}{(\Delta_{af} + \Delta_m * k_H)} \quad \text{Eq. (4.32)}$$

Low pH where find Cl_2

$$J_a = \Delta_{af}^{-1}\left([Cl_2]_f - [Cl_{2(aq)}]_{if}\right) \quad \text{Eq. (4.33)}$$

$$J_m = \Delta_m^{-1}\Delta\left([Cl_{2(aq)}]_m\right) \approx \Delta_m^{-1}\left([Cl_{2(g)}]_f - [Cl_{2(g)}]_s\right) \quad \text{Eq. (4.34)}$$

$$\left([Cl_{2(aq)}]_{if}\right) \approx k_H^{-1}\,[Cl_{2(aq)}]_{if} \quad \text{Eq. (4.35)}$$

$$J_a = \Delta_{af}^{-1} * k_H = [Cl_2]_{if} \quad \text{Eq. (4.36)}$$

$$J_a\,\Delta_{af} = [HClO]_{aq} - J_m\,\Delta_m k_H \quad \text{Eq. (4.37)}$$

Where,

$$J_{af} = J_m$$

$$J * \Delta_{af}\ J * \Delta_m k_H = [Cl_{2(aq)}] \quad \text{Eq. (4.38)}$$

$$J = \frac{[Cl_{2(aq)}]}{\Delta_{af}\ J * \Delta_m k_H} \quad \text{Eq. (4.389)}$$

pH>Cl_2

$$P = \frac{J}{[Cl_{2(aq)}]} = \frac{1}{(\Delta_{af} + \Delta_m * k_H)} \quad \text{Eq. (4.40)}$$

HClO mass balance taking into account separation membrane,

$$2OH^- + Cl_{2(g)} = Cl^- + ClO^- + H_2O \quad K_{RG} \qquad \text{Eq. (4.41)}$$

$$\frac{M_{Cl_2}}{1} = \frac{M_{ClO^-}}{1}$$

$$ClO^- + H_2O \quad K_{RG} \qquad \text{Eq. (4.42)}$$

$$H_2O + Cl_{2(g)} = Cl^- + ClO^- + 2\,H^+ \qquad \text{Eq. (4.43)}$$

$$[HClO]_{TOT} = Cl_{2(g)} = [HClO] + [ClO^-] \qquad \text{Eq. (4.44)}$$

$$K_a = \frac{[H^+] + [ClO^-]}{[HClO]} \rightarrow [ClO^-] = K_a * [HClO][H^+]^{-1} \qquad \text{Eq. (4.45)}$$

For the redox reaction, is defined for $Cl_{2(g)}$ and we want $Cl_{2(aq)}$

$$2H_2O + \cancel{Cl}_{2(g)} = Cl^- + ClO^- + 2\,H^+, \qquad k_1 \qquad \text{Eq. (4.46)}$$

$$Cl_{2(aq)} = \cancel{Cl}_{2(g)} \qquad k^{-1}_{H(Cl_{2(g)})}$$

$$2H_2O + Cl_{2(aq)} = Cl^- + \cancel{ClO^-} + 2\,\cancel{H^+} \qquad \text{Eq. (4.47)}$$

$$\cancel{H^+} + \cancel{ClO^-} = HClO_{aq} \qquad k_a^{-1} \qquad \text{Eq. (4.48)}$$

$$2H_2O + Cl_{2(aq)} = Cl^- + HClO_{aq} + H^+ \qquad k_1 = K_{RG} * k^{-1}_{H(Cl_{2(g)})} + k_a^{-1} \qquad \text{Eq. (4.49)}$$

$$k_1 = \frac{[HClO_{aq}]\,[\,H^+]\,[Cl^-]}{Cl_{2(aq)}} \qquad \text{Eq. (4.50)}$$

$$Cl_{2(aq)} = [HClO_{aq}]\,[\,H^+]\,[Cl^-]{k_1}^{-1} \qquad \text{Eq. (4.51)}$$

$$J_{af} = {\Delta_{af}}^{-1}\left([HClO]_{TOT,f} - [HClO]_{TOT,if}\right) \qquad \text{Eq. (4.52)}$$

$$J_m = {\Delta_m}^{-1}\left([HClO_g]_f + [Cl_{2(g)}]_f + [HClO_g]_s + [Cl_{2(g)}]_s\right) \qquad \text{Eq. (4.53)}$$

Where,

k_{H2O}

$$\left[HClO_g\right]_f = k_{HCl}^{-1}\left[HClO_{aq}\right]_f \quad \text{Eq. (4.54)}$$

K_{HCl2}

$$\left[Cl_{2(g)}\right]_f = k_{HCl}^{-1}\left[HClO_{aq}\right]_f \quad \text{Eq. (4.55)}$$

the k_2,

$$\left[Cl_{2(aq)}\right]_f = \left(\left[HClO_{aq}\right]_f * [\ H^+][Cl^-]{k_1}^{-1}\right) * \left[HClO_{aq}\right]_{if} {k_1}^{-1} \quad \text{Eq. (4.56)}$$

$$J_m * \Delta_m^{-1} = \left(k_{HClO}^{-1} + k_{HCl_2}^{-1}[\ H^+]^{-1}[\ H^+][Cl^-]{k_1}^{-1}\right) * \left[HClO_{aq}\right]_{if} \quad \text{Eq. (4.57)}$$

$$J_m * \Delta_m = \left(k_{HClO}^{-1} + k_{HCl_2}^{-1}1 + [\ H^+][Cl^-]{k_1}^{-1}\right)^{-1} = \left[HClO_{aq}\right]_{if} \quad \text{Eq. (4.58)}$$

$$J_{af} * \Delta_{af} = \left(\left[HClO_{aq}\right] + 1 + k_a[\ H^+]^{-1} + {k_1}^{-1}[\ H^+][Cl^-]\right) - \left[HClO_{aq}\right]_{if} \quad \text{Eq. (4.59)}$$

Where,

$$J_{af} = \Delta_{af}$$

$$J * \Delta_{af} + J * \Delta_m\left(k_{HClO}^{-1} + k_{HCl_2}^{-1}[\ H^+][Cl^-]{k_1}^{-1}\right) \quad \text{Eq. (4.60)}$$

$$J = \frac{1 + k_a[\ H^+]^{-1} + {k_1}^{-1}[\ H^+][Cl^-]}{\Delta_{af} + \Delta_m\left(k_{HClO}^{-1} + k_{HCl_2}^{-1}[\ H^+][Cl^-]{k_1}^{-1}\right)^{-1}}\left[HClO_{aq}\right] \quad \text{Eq. (4.61)}$$

$$P = \frac{1 + k_a[\ H^+]^{-1} + {k_1}^{-1}[\ H^+][Cl^-]}{\Delta_{af} + \Delta_m\left(k_{HClO}^{-1} + k_{HCl_2}^{-1}[\ H^+][Cl^-]{k_1}^{-1}\right)^{-1}} \quad \text{Eq. (4.62)}$$

In summary,

In cases where: $pH > pKa_{HClO} + 1$

$$P = \frac{1 + k_a[\ H^+]^{-1}}{\Delta_{af} + \Delta_m\, k_{HClO}} \quad \text{Eq. (4.63)}$$

In cases where: $pKa_H^+ < pH, pKa_{HClO}+1$

$$P = \frac{1}{\Delta_{af} + \Delta_m \, k_{HClO}} \qquad \text{Eq. (4.64)}$$

In cases where: $pH < pKa_H+1$

$$P = \frac{1 \; + {k_1}^{-1}[\,H^+]\,[Cl^-]}{\Delta_{af} + \Delta_m \left(k_{HClO}^{-1} + k_{HCl_2}^{-1}\,[\,H^+]\,[Cl^-]{k_1}^{-1}\right)^{-1}} \qquad \text{Eq. (4.65)}$$

4.2.6. Determination of the mass transfer coefficient

Gas transfer through the membrane can be expressed by the mass transfer coefficient inside the pore, $k_{Cl.g,pore}$ can be estimated using the correlation of Equations (3.42, 3.43, and 3.44) (Mandowara and Bhattacharya, 2009).

5. RESULTS AND DISCUSSION

In Table 5.1 are shown as example the experimental data collected for one experiment. The complete collections of data generated are shown in the annex chapter. The agitation was constant for all experiments being adjusted to 1000 rpm, the concentrations of chlorine used were 150, 300, and 600 ppm respectively.

Table 5.1. Table data for the results of experiment of 300ppm at pH 1 with FGLP membrane

Time (min)	Brine $V\ Na_2S_2O_3$	NaOH $V\ Na_2S_2O_3$	pH_{Brine}	pH_{NaOH}	C_{brine} (ppm)	C_{NaOH} (ppm)	Losses (%)	Conversion (%)	C'	$\ln(C_i/C_0)$	$\ln(C'/C_0)$
0	1.8	0	0.96	12.915	292.11	0	0.00	0.00	292.11	0.000	0.000
5	1.375	0.125	0.96	12.92	222.90	22.29	16.06	7.63	245.19	-0.270	-0.095
10	1.275	0.225	0.965	12.92	206.62	38.22	16.18	13.08	244.84	-0.346	-0.170
15	1.05	0.3	0.97	12.92	169.98	50.17	24.64	17.17	220.15	-0.541	-0.259
20	0.9	0.35	0.97	12.92	145.56	58.13	30.27	19.90	203.69	-0.697	-0.336
30	0.675	0.425	0.975	12.915	108.92	70.08	38.72	23.99	179.00	-0.987	-0.497
60	0.4	0.6	1.035	12.895	64.14	97.97	44.51	33.54	162.10	-1.516	-0.927
90	0.225	0.7	1.105	12.865	35.64	113.90	48.81	38.99	149.54	-2.104	-1.434
120	0.125	0.8	1.13	12.86	19.35	129.83	48.93	44.45	149.19	-2.714	-2.042

5.1. EVALUATION OF CHLORINE TRANSPORT USING FLAT SHEET MEMBRANES MODULES

5.1.1. FGLP membrane

For the brine solution with initial total chlorine concentration of 300 ppm and pH values from 1 to 7 the highest values of concentration in the receiving solution were measured in in experiments at pH 1, 2 and 4 as it is shown in Figure 5.1. Final total chlorine concentration at the receiving phase at the end of the experiment (120 minutes) was 150 ppm. However, transport rate for more acidic pH solutions decreases with the increase of time. In the experiments removal ratio from the feed to the receiving solution was approximately 50%. .

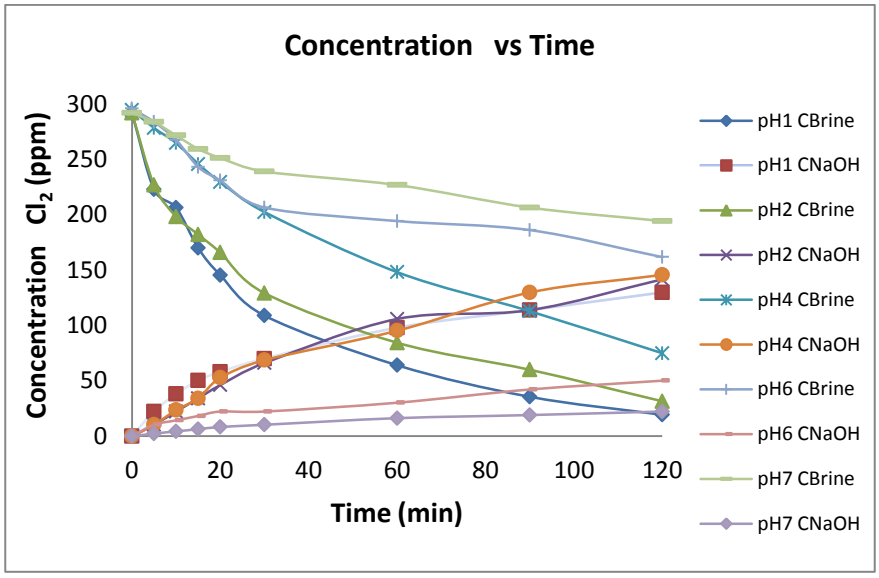

Figure 5.1 Membrane FGLP concentration at 600 ppm in the brine and NaOH compartments at different pH

Experiments carried out with 600 ppm at pH 2 and 6 are shown in Figure 5. For solutions at pH 2 the final chlorine concentration at the receiving phase was 222 ppm (39% of removal ratio). For brines at pH 6 the obtained concentrations at the receiving phase reached a value of 80 ppm after 60 min.

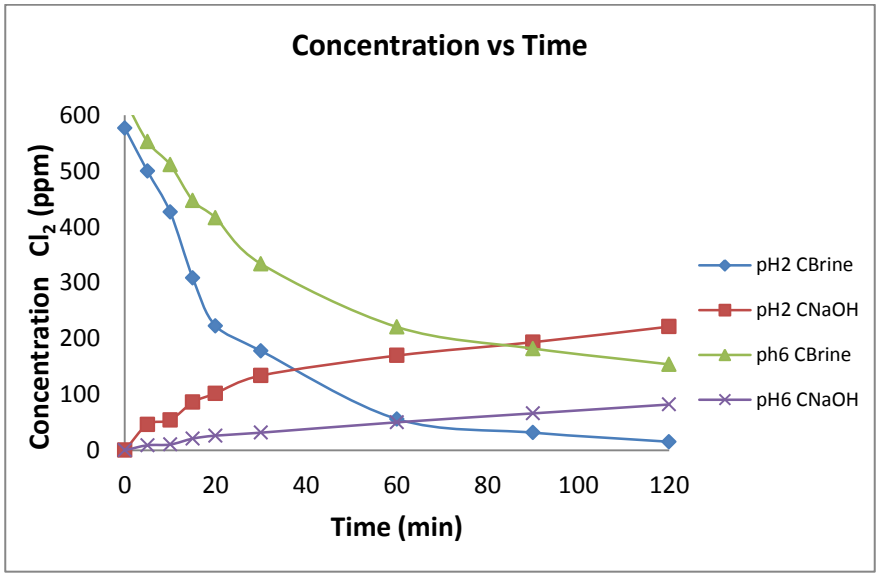

Figure 5.2. . Membrane FGLP concentration at 600 ppm in the brine and NaOH compartments at different pH

For assays at chlorine concentrations of 150 ppm Figure 5.3 shows that at pH 2 the removal ratio reaches 72% of the initial concentration being the more stable transport conditions, this indicates that there very low losses in terms pH 6 was obtained very low concentrations remain constant from 90 minutes.

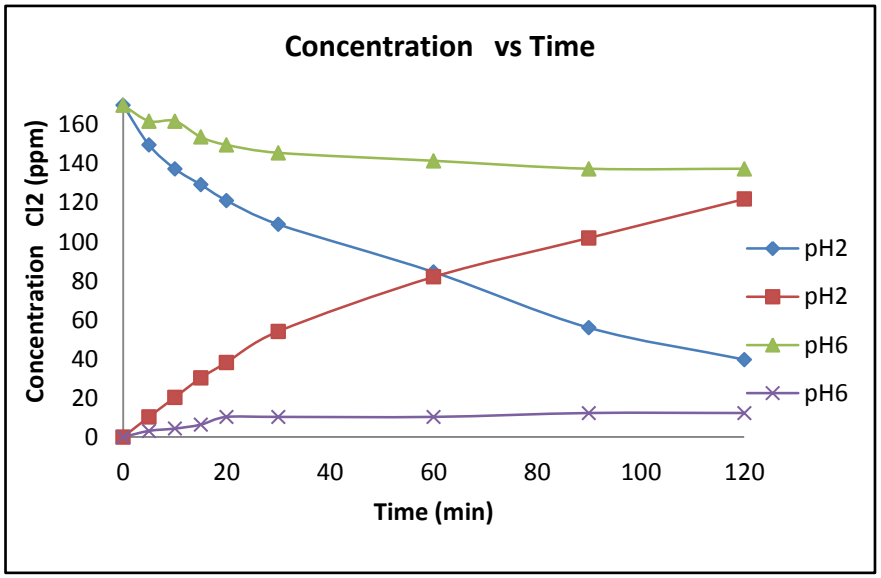

Figure 5.3. Membrane FGLP concentration at 150 ppm in the brine and NaOH compartments at pH 2 and pH 6

Reported losses for all assays, as shown in Figure 5.4, indicates that there is greater loss to pH 1 and pH 2 to 300ppm and 600ppm concentration reaching up to 60%, while for pH 2 150ppm concentrations are low reaching to 5%, losses in concentrations greater than 150ppm, there should be a greater loss when we take the sample, and reason previously mentioned losses are due to leaks module by engines of agitation.

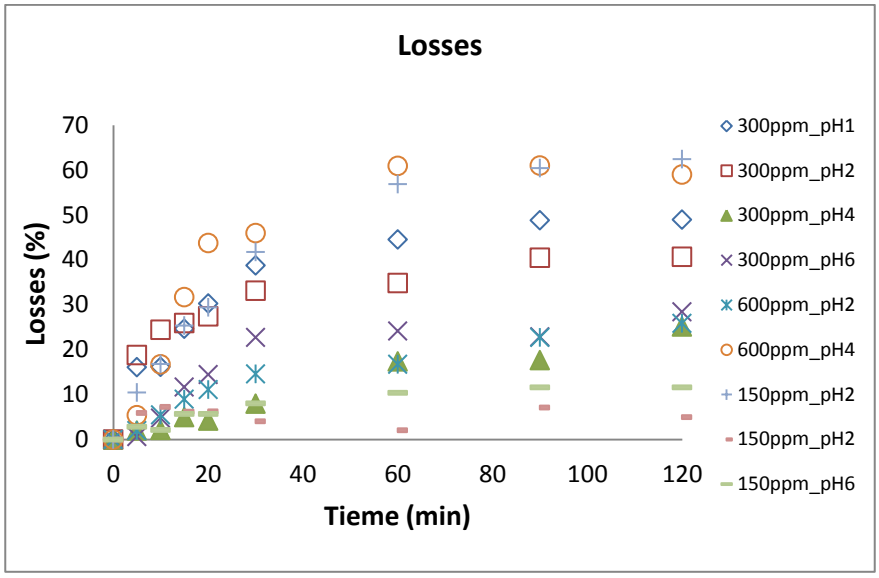

Figure 5.4. Losses at different concentrations and pH in FGLP membrane

Figure 5.5 shows the conversions obtained for all experiments at different pH and initial chlorine concentration, it indicates that the highest conversion was obtained at 150 ppm to pH2 (72%) followed pH 4 (50%) and at 300ppm pH 2 (49%), as explained above for concentrations of 150ppm loss is less and therefore have higher conversion efficiency, whereas the lowest values were obtained for the concentration of 150ppm at pH 6 (6%), 300ppm pH 7 (9%), pH 6 (9%) and 600 ppm pH 6 (9%).

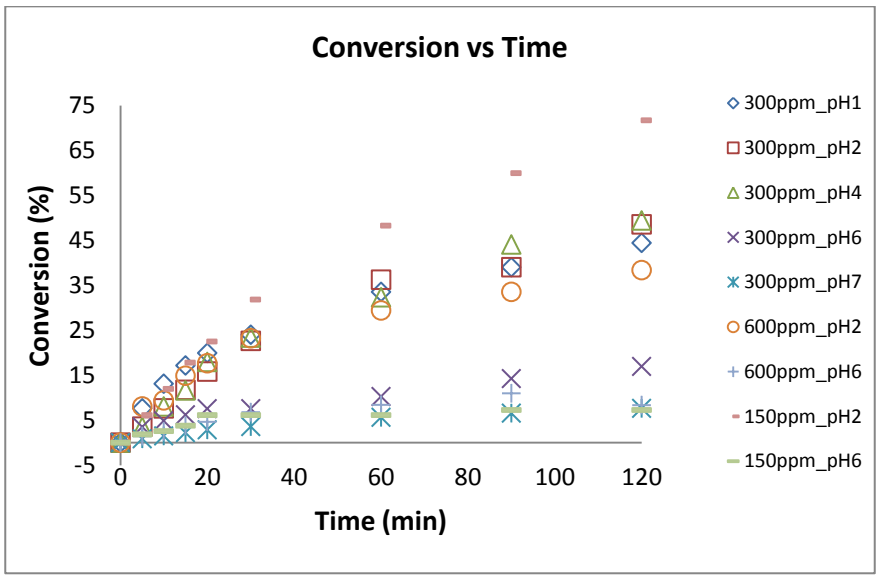

Figure 5.5. Conversion in the receiving solution in FGLP membrane

5.1.2. GVHP membrane

The highest concentrations of gas were determined for pH 1 and pH 2 values as shown in Figure 5.6, for the other pH the concentrations are very low and similar in tendency, which indicates that this type of membrane is differs from the FGLP (Figure 5.1) because there is no significant gas transport at pH 4.

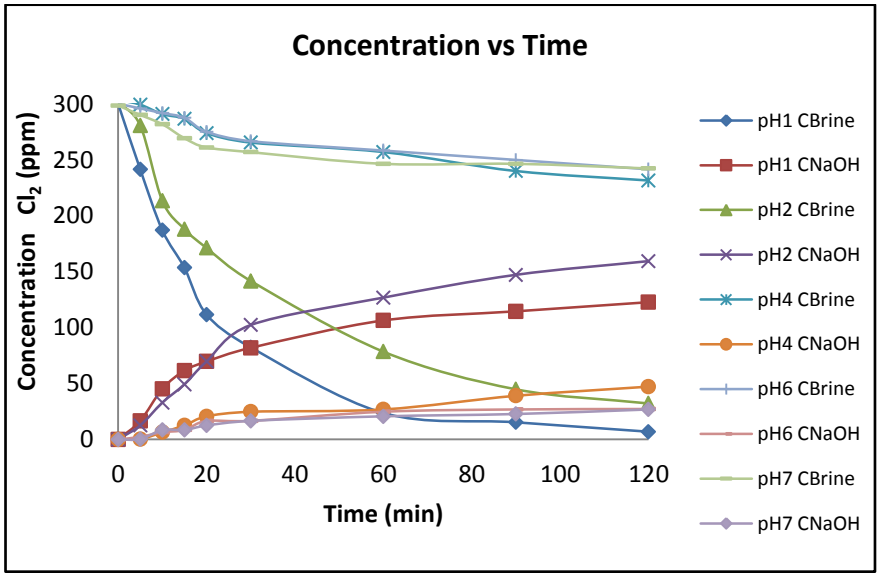

Table 5.6. Membrane GVHP concentrations in the brine and NaOH to 600pmm

Figure 5.7 shows the results obtained for experiments at 600 ppm which is very clearly the difference in final concentrations: 209 and 58 ppm at pH 2 at pH 6 being relatively greater efficiency of the chlorine transport at pH 2.

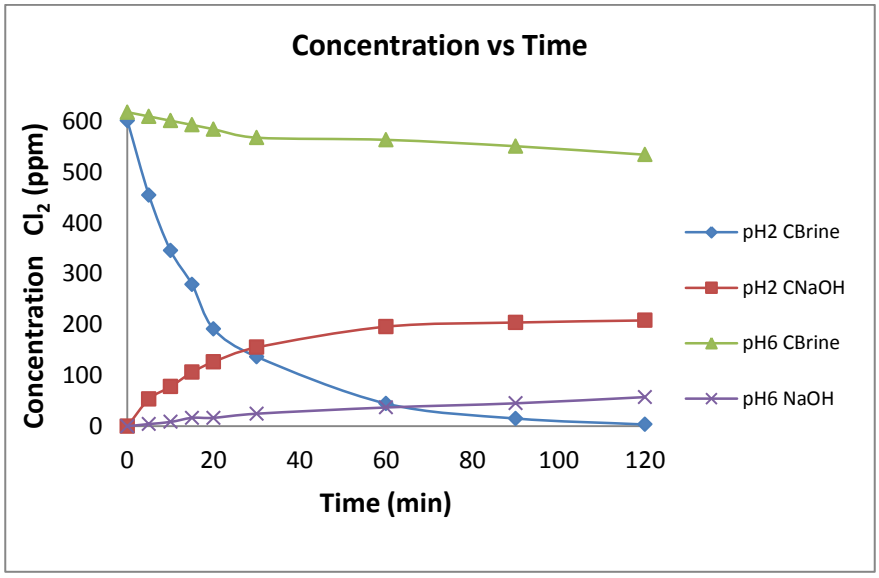

Figure 5.7. . Membrane GVHP concentration at 600 ppm in the brine and NaOH to different pH

The results for concentrations of 150 ppm has the same transport tendency higher concentrations as shown in Figure 5.8, being more effective at pH2 with final concentrations of 58 ppm and very low or poor transport at pH 6 was obtained 8 ppm.

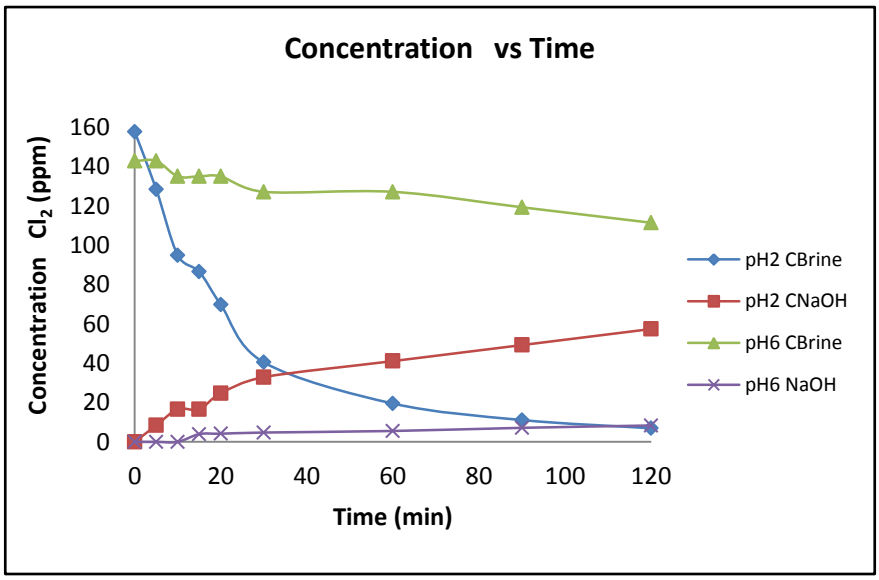

Figure 5.8. Membrane GVHP concentration at 150 ppm in the brine and NaOH to different pH

Results that were obtained for this membrane losses are lower than FGLP membrane, with acceptations concentrations of 300ppm at pH 1 (59%), 600 ppm pH 2 (65%) being those with little difference and a great difference to 150 ppm pH2 (59%), also observed a significant loss

at 300ppm and pH 2 as shown in Figure 5.9 lower losses were determined at 600ppm pH 6 (4%), 300 ppm pH 4 (8%), pH 6 (10%), pH7 (10%) and 150 ppm pH 6 (16%) a can see the all high losses are at low pH (1 to 4) and the low losses are at higher pH.

The higher conversions were obtained for the GVHP membranes at 300ppm of chlorine at pH 1 (41%), pH2 (53%), while for 600 ppm at pH 2 (35%) and for 150ppm at pH 2 (36), being for 300ppm and pH 2 the best conditions for chlorine transport. The chlorine transport percentage for 150 ppm and pH6 the lower values were obtained (6%) followed by those at 300ppm and pH 7 (9%) and very similar at pH6 (9%) as could be seen in Figure 5.8.

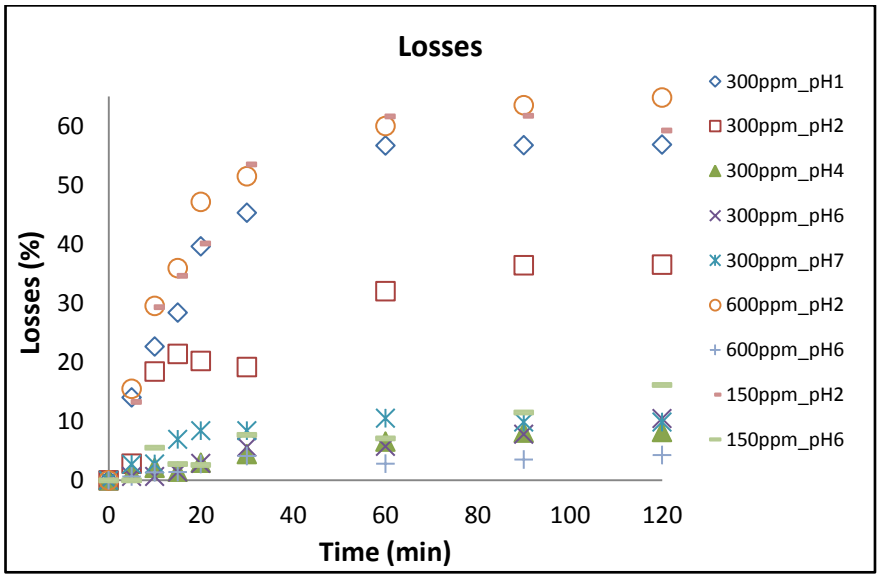

Figure 5.9. Losses at different concentrations and pH in FGLP membrane

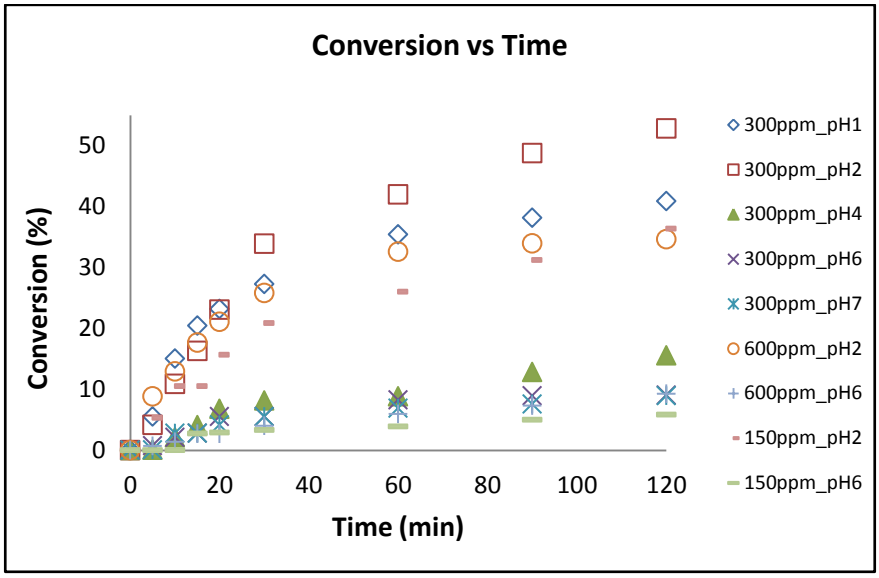

Figure 5.10. Conversion in the receiving solution in FGLP membrane

5.2. DETERMINATION OF MEMBRANE PERMEABILITY FOR CHLORINE SPECIES

For determinations of the membranes permeability to chlorine transport the mass balance equations were used when significant losses were measured. The linearization of the experimental data in the form of [ln(C/C_0) vs time] was used to determine the permeability by using the Equation (4.9)

$$C_0 = C_t^B + C_t^{NaOH} \qquad \text{Eq. 4.66}$$

$$C_0 = C_t^B + C_t^{NaOH} + C_t^L \qquad \text{Eq. 4.67}$$

$$\ln\frac{C_0 - C_t^L}{C_t^B} = \ln\frac{C_0 - C_0 + C_t^B + C_t^{NaOH}}{C_t^B} = \ln\frac{C_t^B + C_t^{NaOH}}{C_t^B} \qquad \text{Eq. 4.68}$$

$$\ln\frac{C_t^B + C_t^{NaOH}}{C_t^B} = \frac{P_i * A * t}{V} \qquad \text{Eq. 4.66}$$

Figure 5.11 shows the membrane permeability values of FGLP and GVHP membranes for all concentrations studied. It could be seen that the an increase in the permeability takes place in the membrane GVHP at 300ppm concentration condition at pH1 and pH 2 followed by 600ppm for the same membrane. The values determined for each membrane under the different experimental conditions are shown in Table 5.2.

Table 5.2. Permeability of the membranes FGLP and GVHP to different concentrations and pH

pH	FGPL ($cm.s^{-1}$)			GVHP ($cm.s^{-1}$)		
	300ppm	**600ppm**	**150ppm**	**300ppm**	**600ppm**	**150ppm**
1	1.22E-03	-	-	3.11E-03	-	-
2	1.01E-03	1.72E-03	8.52E-04	1.13E-03	2.47E-03	1.41E-03
4	6.52E-04	-		2.74E-04		
6	1.48E-04	2.67E-04	8.15E-05	2.07E-04	5.92E-05	4.44E-05
7	6.67E-05	-	-	1.63E-04	-	-

For a better description of the membrane permeability values with respect to the pH shown in Figure 5.11, in the range $4.44x10^{-5}$ to $2.67x10^{-4}$ $cm.s^{-1}$ for both membranes at pH 6 and pH 7 a magnification of these values was included in the figure.5.9 It could be seen that in the membrane FGLP at 150ppm pH 1, 300ppm pH 7 and GVHP at 150ppm pH 6 and 600ppm pH6 permeability values are very close to each other, thus confirming that both membranes at different initial concentration and pH 6 are very similar permeability.

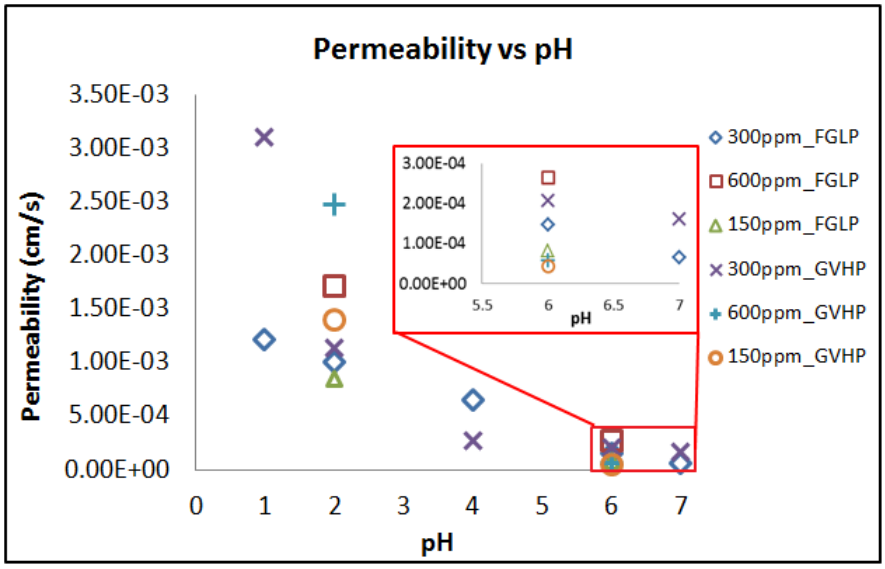

Figure 5.11. Permeability behavior with pH in FGLP and GVHP membrane

Higher permeability occurs with the GVHP membrane for working conditions of 300 ppm of chlorine and pH 1 ($3.11x10^{-3}$ $cm.s^{-1}$) as shown in Figure 5.11, followed by 600 ppm at pH 2 ($2.47x10^{-3}$ $cm.s^{-1}$). For the FGLP membrane for 600 ppm of total chlorine at pH 2 a permeability alues of $1.72x10^{-3}$ $cm.s^{-1}$ was measured. For lower total initial chlorine concentrations permeability values ranged from $4.44x10^{-5}$ to $2.67x10^{-4}$ $cm.s^{-1}$. At basic pH values (6 and 7) both membranes provided similar permeability values.

5.3. CALCULATION OF DIFFUSIVITY AND MASS TRANSFER COEFFICIENT OF CHLORINE SPECIES

For the determination of diffusivity is was used the Henry's constant 0095mol/m^3.atm (Lide and Frederikse, 1995) and converted into dimensionless constant and using the relation: mass transfer coefficient in the interface brine (k_{af}) equal to the diffusivity of the membrane (equal to the diffusion coefficient of chlorine in dilute solutions) divided by the thickness of the membrane as see Equation (4.69), in this way determine the mass transfer coefficient in the interface and substituting in Equation (4.21), it is deducted that considering that the flow of the membrane is equal to the mass transfer coefficient in the membrane was obtained with this diffusivity data and then determine the mass transfer coefficient inside the pore.

The behavior of diffusivity with respect to the initial concentration used and pH established was determined: higher diffusivity are reported in the GVHP membrane at 300ppm and pH1

(7.23x10^{-3} cm^2.s^{-1}) and a pH 600ppm (2 5.75x10^{-3} cm^2.s^{-1}) as we can see in Table 5.3, while the intermediate values as seen in Figure 5.12 intervals were between 1.51 x10^{-3} to 2.63 x10^{-3} cm^2.s^{-1} in terms of low values have to pH6 and pH7 are relatively similar for the two membranes studied, it is noteworthy that the lower value is reported at 150ppm pH6 in the GVHP membrane (1.03 x10^{-4} cm^2.s^{-1}).

To calculate the mass transfer coefficient inside de pore were used the Equations (3.42) and (3.43), this is a correlation (Mandowara and Bhattacharya, 2009), use this correlation to determine the tortuosity which is the division of the unit for membrane porosity squared, also the membrane thickness data. The porosity and thickness values are different in both membranes. The highest value of mass transfer coefficient is GVHP membrane in condition at 300ppm pH1 (5.31x10^{-5}cm.s^{-1}) and the lower coefficient 150ppm pH6 (7.59 x10^{-7}cm.s^{-1}) in the same membrane.

$$k_{af} = \frac{1}{\Delta_{af}} = \frac{D_{af}}{d} \qquad \text{Eq. (4.69)}$$

Table 5.3. Diffusivity studies for the GVHP and FGLP membranes

pH	FGPL (cm^2.s^{-1})			GVHP (cm^2.s^{-1})		
	300ppm	**600ppm**	**150ppm**	**300ppm**	**600ppm**	**150ppm**
1	2.84E-03	-	-	7.23E-03	-	-
2	2.34E-03	3.99E-03	1.98E-03	2.63E-03	5.75E-03	3.27E-03
4	1.51E-03	-	-	6.37E-04	-	-
6	3.44E-04	6.20E-04	1.89E-04	4.82E-04	1.38E-04	1.03E-04
7	1.55E-04	-	-	3.79E-04	-	-

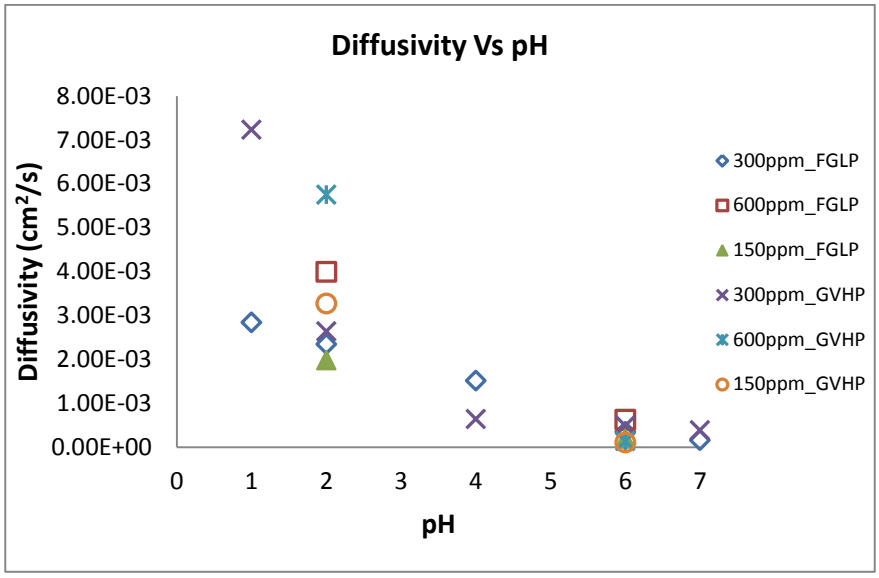

Figure 5.12. Diffusivity behavior with pH in FGLP and GVHP membrane

The behavior of diffusivity with respect at the initial total chlorine concentration and pH determined the higher diffusivity values for the GVHP membrane at 300 ppm pH 1 ($7.23x10^{-3}$ $cm^2.s^{-1}$) and at pH 600 ppm pH 2 ($5.75x10^{-3}$ $cm^2.s^{-1}$), while intermediate values, as shown in Figure 5.12 , between $1.51x10^{-3}$ to $2.63x10^{-3}$ $cm^2.s^{-1}$ were measured for solutions at higher pH (6 and 7). These values are comparatively similar for the two membranes studied. It should be mentioned that the lowest value measured for total chlorine concentrations of 150 ppm at pH 6 with in GVHP membrane ($1.03x10^{-4}$ $cm^2.s^{-1}$) as we can see in Table 5.3

The mass transfer coefficient is calculated from the diffusivities obtained using equations 3.42 and 3.43. The highest value of mass transfer coefficient was obtained for GVHP membranes at 300 ppm at pH 1 ($5.31x10^{-5}$ $cm.s^{-1}$) and followed at 600 ppm at pH 2 ($4.23x10^{-5}$ $cm.s^{-1}$). For the case of FGLP membrane lower coefficients were determined for 150 ppm at pH 6 ($7.59x10^{-7}$ $cm.s^{-1}$).

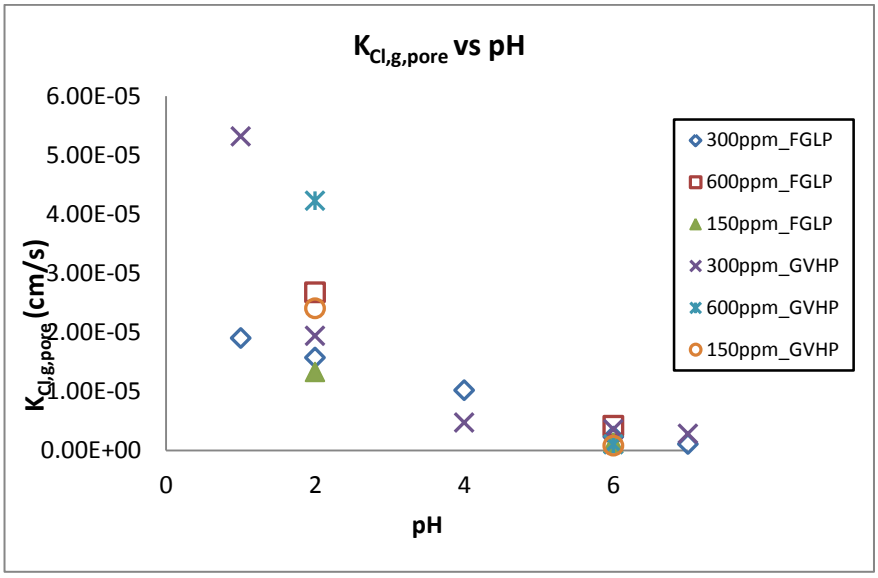

Figure 5.13. Mass transfer coefficient inside de pore with pH in FGLP and GVHP membrane

5.4. MEMBRANE CHARACTERIZATION

Membranes used were characterized using the Fourier Transform Infrared Spectrophotometer (FT-IR) and Scanning Electron Microscope and Energy Dispersive X-Ray Spectrometer (SEM-EDS.SEM was used to study the membrane surface morphology and to determine the elemental composition of the membrane surface and potential deposits on the membrane surface. FTIR analysis was done to find the type of deposits on the membrane surface (define the structure). FTIR give a series of peaks, which depicts the qualitative values of various constituents on the membrane surface.

Samples to be analyzed and characterized of virgin and used membrane carried out the FT-IR. This technique required that the membrane should be completely dry to avoid the interference in peaks presented by water.

A membrane used in the module was divided in four equal parts and then were placed in 5% solution of sodium hydroxide, 300ppm NaClO (Brine), HCL pH 1 and pH 4 for a time of 12 weeks for the membrane GVHP and 6 weeks for FGLP and compared with a virgin membrane.

Infrared spectra were obtained from 550 to 4000 cm^{-1} the identified spectrum region in the membrane FGLP is important information on the conformational isomerism of the chain is providing information as shown in Table 5.4.

Changes were observed in comparison with the virgin membrane and the samples after interacting with brine solutions at 300ppm NaOCl, HCL to pH 1, pH 4 and 5% NaOH as shown in Figure 5.14.

Table 5.4 Observed frequencies cm^{-1}: characteristic bands with specific vibrational of the virgin membrane and after interacting with NaClO, HCl, NaOH solutions.

Membrane FGLP						
VIRGIN	**NaClO 300ppm**	**HCl pH1**	**HCl pH4**	**NaOH 5%**	**Group**	**Vibration**
2913	2914	2914	2914	2914	CH2, CH3	Stretching
2847	2847	2847	2847	2847		
1470	1469	1469	1469	1469	CH2, CH3	Deformation
-	1215	1214	-	1218	CF2	Symmetric stretching
-	1055	1155	-	1154	CF3	Symmetric stretching
-	-	1047	-	1046	CF3	Symmetric stretching
717	717	717	716	717	CF2	Scissoring
580	580	579	559	592	CF3	Symmetric deformation (umbrella)
567	567	562	562	577	CF2	Bending

Only three new bands were detected for the HCl pH 1 (1407- 1155 -1214cm^{-1}), %5 NaOH (1046 -1054 -1218 cm^{-1}), one for NaClO 300ppm (1055 - 1215 cm^{-1}) these spectral changes can be explained by modifications of the polymer chain or side group; been shortened (broken), leading to the formation of more and more CF3 ending groups. (Mihály, J. et al 2006).

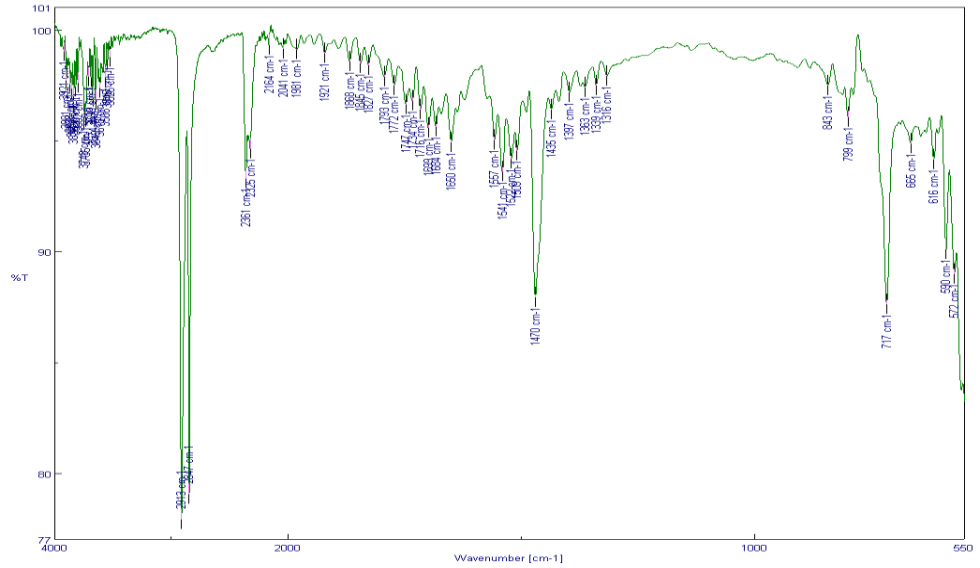

(a)

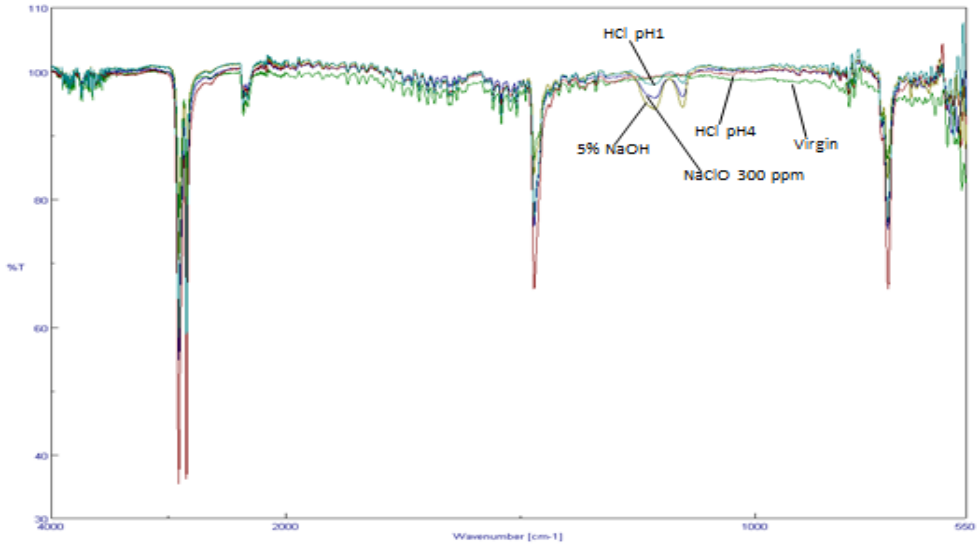

(b)

Figure 5.14. FTIR spectra of FGLP membrane. (a) virgin membrane and (b) spectra of different samples virgin membrane and after interacting with solutions of chemicals NaClO, HCl, NaOH.

Table 5.5. Observed frequencies (cm^{-1}) of the IR spectra of the virgin membrane and aged membranes with solutions of chemicals NaClO, HCl, NaOH.

Membrane GVHP						
VIRGIN	**NaClO 300ppm**	**HCl pH1**	**HCl pH4**	**NaOH 5%**	**Group**	**Vibration**
1402	1402	1402	1402	1402	CH2	Stretching
1178	1178	1179	1179	1178	CF2	Symmetric stretching
874	874	874	874	874		CH2 Asymmetric stretching and CF2 asymmetric stretching
764	764	764	764	764	CF2, CCC	
677	677	677	667	665		In-plane bending or rocking
614	614	614	613	614	CF2, CCC	Bending and CCC skeletal vibration
564	560	569	552	563	CF2	Bending

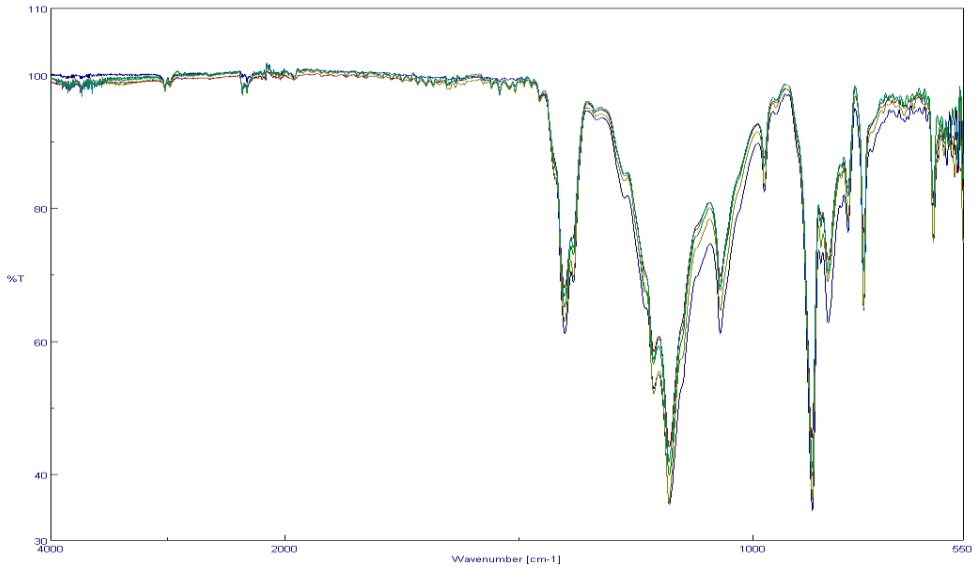

Figure 5.12. FTIR spectra of GVHP membrane under different experimental conditions: virgin membrane and after interacting with solutions of chemicals NaClO, HCl, NaOH.

From the Table 5.4 for FGLP membrane it was identified CH2 asymmetric, CH2 asymmetric and CH2 deformation peaks assigned to the bands 2913, 2847cm^{-1} and 1470 cm^{-1} respectively. The strong band at 1470cm^{-1} is assigned a deformation of CH2, in the interval 1214 -1218cm^{-1} is assigned CF2 Symmetric stretching, 1046 - 1218cm^{-1} assigned to the CF2-CF3 symmetric stretching and 717cm^{-1} assigned CF2 scissoring, 508-592cm^{-1} CF3 with symmetric deformation in umbrella and 580 - 592cm^{-1} CF2 Bending, this assignations. In fact there has been reported are very similar values in a previous study of PDVF membrane (Mihály, J. et al 2006).

At has been reported previously the presence of three new bands, shown in Table 5.4, can be explained by modifications of the polymer chain or side group (CF2 and CF groups) (Mihály, 2006; Drage, 2006). Finally the new band at 1154-1218cm^{-1} may correspond to bromotrifluoromethane (CF_3Br).

FTIR data for the GVHP membrane shown no significant changes in the frequencies as shown in the Table 5.4 and Figure 5.15 meaning that no absorption (reaction) or almost null degradation the membrane by the solution. This was also confirmed by the SEM images as can see Figures 5.16 and 5.17.

FTIR assignments for the GVHP membranes (virgin and aged) were: 1042 cm^{-1} CH2 Stretching, 1178 - 179 cm^{-1} CF2 symmetric stretching, 685 - 874 cm^{-1} CH2 asymmetric stretching and CF2 asymmetric stretching 613 - 614 cm^{-1} bending and CCC skeletal vibration and 552 - 564 cm^{-1} bending. Minimum changes were detected when compared both virgin and aged samples as has been previously reported by Nallasamy (Nallasamy, 2006).

Scanning Electron Microscope (SEM) was used for characterization of the surface of the membranes to identify potential modifications of the structure of the membrane under the acidic and oxidizing conditions evaluated or the potential precipitation or deposition of solids during the operation of the hydrophobic membranes.

As seen in the Figure 5.16 (a) and (b) FGLP membrane virgin sample unchanged while the membrane used for the transportation of chlorine presents incrustations in accordance with the graph 5.17, these encrustations are magnesium and silicon. The Figure 15.16 (b) shows that there is some degree of breaking the membrane structure.

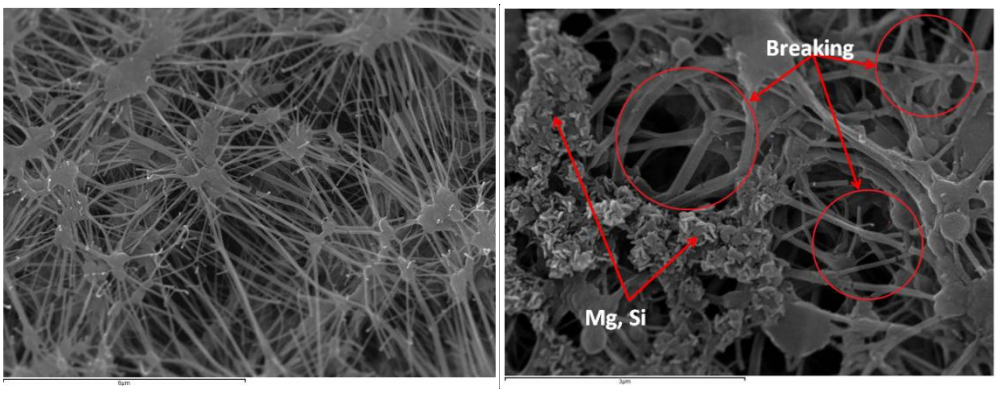

Figure 5.16. SEM images of the surface of FGLP membrane (a) virgin membrane (10x); (b) after interacting with brine (20k)

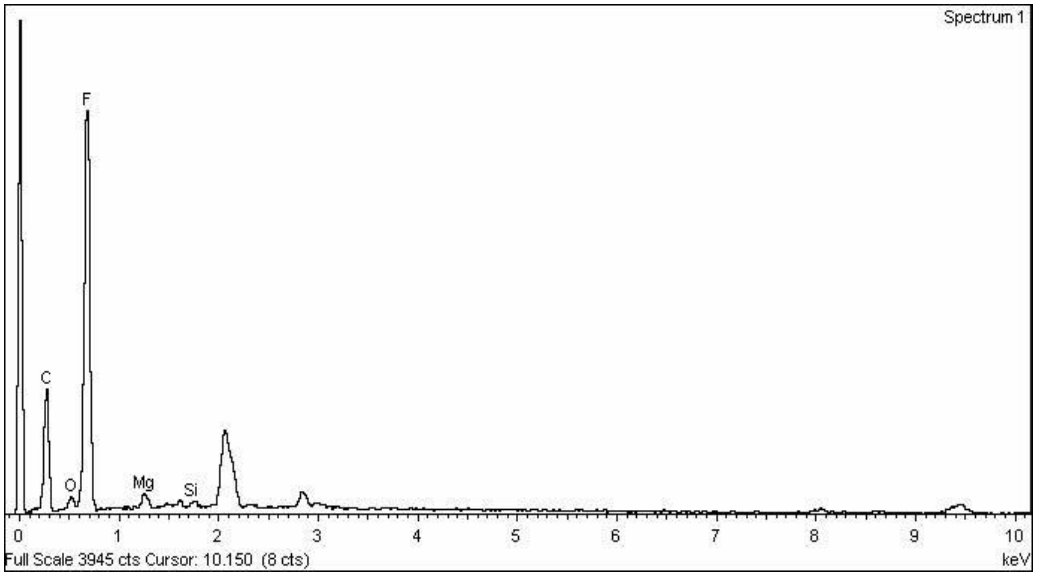

Figure 5.17. EDS of the surface of FGLP after interacting with brine

The electron microscope photographs and the EDS analysis show no change in the structure of the GVHP membrane sample which indicates that it is inert to attack by acidic or basic solutions, we can see in Figure 5.18 (b) and 5.19

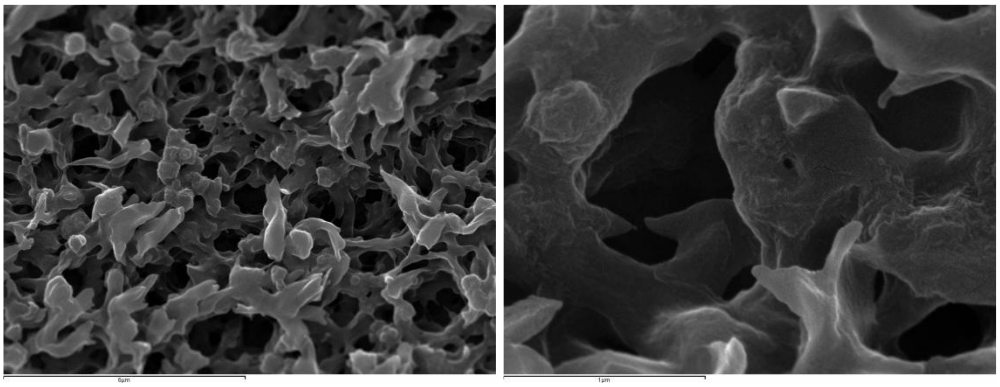

(a) **(b)**

Figure 5.18. SEM images of the surface of GVHP membrane (a) virgin membrane (10x); (b) after interacting with brine (50x)

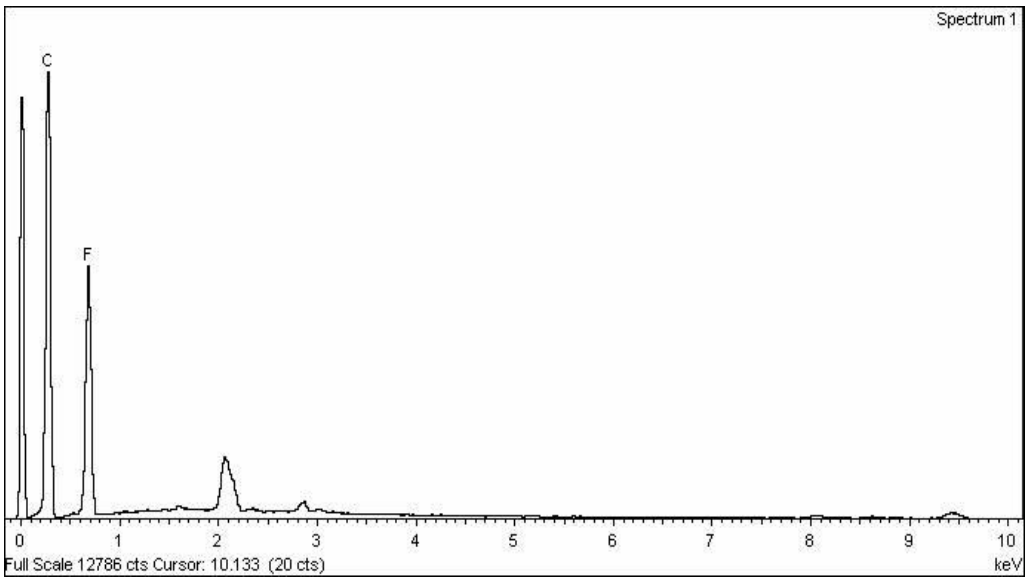

Figure 5.19. EDS of the surface of GVHP after interacting with brine

6. CONCLUSIONS

The research work shows the following conclusions from the results of the experiments in this study:

a) Fluoride base polymeric hydrophobic membranes Polytetrafluoroethylene (FGLP) and (Polyvinylidene fluoride (GVHP) are suitable materials for the transport of chlorine species from sodium chloride brines.

b) The experimental results at different pH values indicate that for both membranes both HOCl(g) and Cl_2(g) species are transported efficiently.

c) Polyvinylidene fluoride (GVHP) bases membranes give the highest permeability values up to $3.1x10^{-3}$ $m.s^{-1}$ in the operating conditions evaluated and the permeability depends directly on the acidity of the brine solutions.

d) Chlorine transport results shown that the best operating conditions were achieved for the most acidic conditions evaluated of pH. In this high acidic and oxidizing conditions the membrane is highly resistant to the potential chemical degradation attacks of the feed solution and the receiving solution.

e) Mass transport coefficients values from $7.59x10^{-7}$ to $5.31x10^{-5}$ $cm.s^{-1}$ were measured for GVHP membranes while for the FGLP membrane those varied from $1.27x10^{-6}$ to $1.90x10^{-5}$ $cm.s^{-1}$.

However, many research and development efforts are necessary to develop a new technology of the chlorine purification using this type of membranes in liquid-liquid contactors.

7. REFERENCES

AENOR. Productos químicos utilizados en el tratamiento del agua destinada al consumo humano: Hipoclorito de sodio. UNE-EN 901. Madrid: AENOR, 2007.

Agrahari, G. K., Verma, N., Bhattacharya P.K., 2011. Application of hollow fiber membrane contactor for the removal of carbon dioxide from water under liquid–liquid extraction mode, Journal of Membrane Science 375, 323–333.

Al-Marzouqi, M.H., El-Naas, M.H., Marzoukb, S.A.M., Al-Zarooni, M.A., Abdullatif, N., Faiz, R., 2008. Modelling of CO absorption in membrane contactors. Separation and Purification Technology 59, 286-293.

Baker, R.W., Cussler, E. L., Eykamb, W., Koros, W. J., Riley, R. L., Strathmann H., Membrane Separation Systems: Recent Development and Future Directions, Noyes Data Corporation, 1991.

Bitter, J. G. A. , 1991 Transport Mechanisms in Membrane Separation Processes, Plenum Chemical Engineering Series, Plenum Press.

Bommaraju, T. J., Orosz, P. J., Sokol, E. A., 2007, BRINE ELECTROLYSIS: Electrochemistry Encyclopedia http://electrochem.cwru.edu/encycl

Boyadzhiev, L. and Lazarova, Z., Liquid Membranes, Chapter 7 in “Membrane Separations Technology: Principles and Applications”, Membrane Science and Technology Series, eds. R. A. Noble and S. A. Stern, Elsevier, 1995.

Cen, Y. and Lichtentharler, R. N. Vapor Permeation, Chapter 3 in “Membrane Separations Technology: Principles and Applications”, Membrane Science and Technology Series, eds. R. A. Noble and S. A. Stern, Elsevier, 1995.

ÇENGEL, Yunus A. Heat and mass transfer: a practical approach. 3th edition. Mexico, McGraw-Hill, 2007. 901 pag. McGraw-Hill series in mechanical and aerospace engineering. ISBN007325035X

Deborde, M., Gunten, U., 2008, Reactions of chlorine with inorganic and organic compounds during water treatment-Kinetics and mechanisms: A critical review, Water Res. 42, 13-51.

Deborde, M., von Gunten, U., 2008, Reactions of chlorine with inorganic and organic compounds during water treatment - kinetics and mechanisms: a critical review, Journal of Water Research, 42, 13-51.

Directiva 98/83/CE del Consejo del 3 de noviembre de 1998 relativa a la calidad del agua destinada al consumo humano.

Drage E.A., Jaksch, D., Smith, K.M. McPheat, R.A. Vasekova, E., Mason N.J.(2006). FTIR spectroscopy and estimation of the global warming potential of CF3Br and C2F4, Journal of Quantitative Spectroscopy and Radiative Transfer, Volume 98, Issue 1, Pages 44–56

Eurochlor, magazine, 2011, Nº 10, Chlorine Industry Review 2010-2011: http://www.eurochlor.org/download-centre/the-chlorine-industry-review.aspx

Eykamp, W., Microfiltration and Ultrafiltration, Chapter 1 in “Membrane Separations Technology: Principles and Applications”, Membrane Science and Technology Series, eds. R. A. Noble and S. A. Stern, Elsevier, 1995.

Fell, C. J. D., Reverse Osmosis, Chapter 4 in “Membrane Separations Technology: Principles and Applications”, Membrane Science and Technology Series, eds. R. A. Noble and S. A. Stern, Elsevier, 1995.

Gallard, H., Pellizzari, F., Croue., J.P., Legube, B., 2003. Rate constants of reactions of bromine with phenols in aqueous solution. Water Res. 37, 2883–2892.

Hägg, M.-B., 2000, Membrane purification of Cl2 gas. I. Permeabilities as a function of temperature for Cl2,O2,N2,H2 in two types of PDMS membranes, J. Membr. Sci. 170, 173-190.

Hägg, M.-B., 2000, Membrane purification of Cl2 gas. II. Permeabilities as a function of temperature for Cl2,O2,N2,H2 and HCl in perfluorinated, glass and carbon molecular sieve membranes, J. Membr. Sci. 177, 109-128.

Hägg, M.-B., 2009, Membrane separation of chlorine gas, J. Membr. Sci., 48,1–16.

Hasanoglu A. Romero J. Pérez B. Plaza A. 2010. Ammonia removal from wastewater streams through membrane contactors:Experimental and theoretical analysis of operation parameters and configuration, Chem. Eng. J. 160, 530–537.

Huthwelker, T.; Clegg, S.L.; Peter, T.; Carslaw, K.; Luo, B.P.; Brimblecombe, P. 1995. Solubility of HOCl in water and aqueous H2SO4 to stratospheric temperatures, J. Atmos. Chem., 21, 81-95.

Javaid, A., 2005. Membranes for solubility-based gas separation applications, Chem. Eng. J. 112, 219-226.

Keshavarz, P., Fathikalajahi, J., Ayatollahi, S., 2008a. Mathematical modelling of the simultaneous absorption of carbon dioxide and hydrogen sulphide in a hollow fibre membrane contactor. Separation and Purification Technology 63, 145-155.

Kieffer, R., Charcosset, C., Puel, F., Mangin, D., 2008. Numerical simulation of mass transfer in a liquid-liquid membrane contactor for laminar flow conditions. Computers and Chemical Engineering 32, 1325-1333.

Lahoutifard, N., Lagrange, P., Lagrange, J., 2003. Kinetics and mechanism of nitrite oxidation by hypochlorous acid in the aqueous phase. Chemosphere 50, 1349–1357.

Lide and Frederikse, 1995. CRC Handbook of Chemistry and Physics, 76th Edition, D. R. Lide and H. P. R. Frederikse, ed(s)., CRC Press, Inc., Boca Raton, FL.

Lindbråthen, A., Hägg, M.-B., 2005. Glass membranes for purification of aggressive gases. Part II. Adsorption measurements and diffusion coefficient estimations, J. Membr. Sci. 259, 154-160.

Lindbråthen, A., Hägg, M-B., 2009. Membrane separation of chlorine gas Chemical Engineering and Processing 48, 1-16.

Mandowara, A., Bhattacharya, P., 2011. Simulation studies of ammonia removal from water in a membrane contactor under liquid-liquid extraction mode, Journal of Environmental Management 92, 121-130.

Mandowara, A., Bhattacharya, P.K., 2009. Membrane contactor as degasser operated under vacuum for ammonia removal from water: a numerical simulation of mass transfer under laminar flow conditions. Computers and Chemical Engineering 33, 1123-1131.

Mihály, J., Sterkel, S. Ortner, H., Kocsis, L., Furdyga, É., Hajba,L., Mink, J. 2006. FTIR and FT-Raman Spectroscopic Study on Polymer Based High Pressure Digestion Vessels, 79 (3) 497-501.

Nallasamy p., Mohan S., 2005. Vibrational Spectroscopy characterization of form II poly (vinylidene fluoride), Indian Journal of Pure & Applied Physics, 43, 821-826.

Norddahl, B., Horn, V.G., Larsson, M., Preez, J.H., Christensen, K., 2006. A membrane contactor for ammoniastripping, pilot scale experience and modeling, Desalination 199, 172–174.

White, G. C., & Black & Veatch. 2010. White's handbook of chlorination and alternative disinfectants. Hoboken, N.J: Wiley.

WHO (2003) Bromate in drinking-water. Background document for preparation of WHO Guidelines for drinking-water quality. Geneva, World Health Organization (WHO/SDE/WSH/03.04/78).

WHO (2005a) Bromate in drinking-water. Background document for development of WHO Guidelines for drinking-water quality. Geneva, World Health Organization (WHO/SDE/WSH/05.08/78; WHO/HSE/WSH/09.04/54; http://www.who.int/water_sanitation_health/dwq/chemicals/en/).

WHO (2011) Guidelines for drinking-water quality, 4th ed. Geneva, World Health Organization.

World Health Organization, 2001, Safe drinking-water from desalination, http://www.who.int/water_sanitation_health/publications/2011/desalination_guidance/en/index.html

Yu, P., Kirkpatrick, J. Poe B, McMillan, P. F., Cong, X. 1999. Structure of Calcium Silicate Hydrate (C-S-H): Near-, Mid-, and Far-Infrared Spectroscopy, J. Am. Ceram. Soc., 82 [3] 742–48.

Zhu, Z., Hao, Z., Shen, Z., Chen,J. 2005. Chen, Modified modeling of the effect of pH and viscosity on the mass transfer in hydrophobic hollow fiber membrane contactors,J. Membr. Sci. 250, 269–276.

ANNEX

A.1. DATA TABLE FOR THE FGLP MEMBRANE

Calculation of chlorine concentration

Table 1. Chlorine concentration of FGLP membrane at 300ppm

Time (min)	pH1		pH2		pH4		PH6		pH7	
	C_{brine} (ppm)	C_{NaOH} (ppm)	C_{brine} (ppm)	C_{NaOH} (ppm)	C_{brine} (ppm)	C_{NaOH} (ppm)	C_{brine} (ppm)	C_{NaOH} (ppm)	C_{brine} (ppm)	C_{NaOH} (ppm)
0	292.11	0	292.11	0	294.83	0	296.18	0.00	292.11	0.00
5	222.90	22.29	226.98	10.34	278.54	10.34	283.97	10.34	283.97	2.37
10	206.62	38.22	198.48	22.29	264.97	23.61	267.69	14.32	271.76	4.36
15	169.98	50.17	182.19	34.24	245.97	34.24	243.26	18.30	259.54	6.35
20	145.56	58.13	165.91	46.18	229.69	52.82	231.05	22.29	251.40	8.34
30	108.92	70.08	129.27	66.10	202.55	68.76	206.62	22.29	239.19	10.34
60	64.14	97.97	84.49	105.93	148.27	95.31	194.41	30.25	226.98	16.31
90	35.64	113.90	60.06	113.90	112.99	129.83	186.27	42.20	206.62	19.10
120	19.35	129.83	31.57	141.78	74.99	145.77	161.84	50.17	194.41	22.29

Table 2. Chlorine concentration of FGLP membrane at 600ppm

Time (min)	pH2		PH6	
	C_{brine} (ppm)	C_{NaOH} (ppm)	C_{brine} (ppm)	C_{NaOH} (ppm)
0	577.08	0	627.22	0
5	499.73	46.18	552.62	9.01
10	426.45	54.15	511.47	10.34
15	308.40	86.02	447.16	20.96
20	222.90	101.95	416.29	26.27
30	178.12	133.82	333.97	31.58
60	55.99	169.67	220.79	50.17
90	31.57	193.57	182.21	66.10
120	15.28	221.45	153.91	82.03

Table 3. Chlorine concentration of FGLP membrane at 150ppm

Time (min)	pH2		PH6	
	C_{brine} (ppm)	C_{NaOH} (ppm)	C_{brine} (ppm)	C_{NaOH} (ppm)
0	169.98	0	169.98	0
5	149.63	10.34	161.84	3.17
10	137.41	20.29	161.84	4.36
15	129.27	30.25	153.70	6.35
20	121.13	38.22	149.63	10.34
30	108.92	54.15	145.56	10.34
60	84.49	82.03	141.48	10.34
90	55.99	101.95	137.41	12.33
120	39.71	121.87	137.41	12.33

Calculation of chlorine losses

Table 4. Losses in the FGLP membrane

Time (min)	300 ppm					600 ppm		150 ppm	
	pH1	pH2	pH4	pH6	pH7	pH2	pH6	pH2	pH6
0	0.00	0.00	0.00	0.00	0.00	0.00	0.00	0.00	0.00
5	16.06	18.76	2.02	0.63	1.98	5.40	10.46	5.89	2.85
10	16.18	24.42	2.12	4.79	5.48	16.72	16.81	7.22	2.14
15	24.64	25.91	4.96	11.69	8.97	31.65	25.37	6.15	5.69
20	30.27	27.39	4.18	14.47	11.08	43.71	29.44	6.26	5.69
30	38.72	33.12	7.98	22.71	14.58	45.95	41.72	4.07	8.06
60	44.51	34.81	17.38	24.15	16.71	60.90	56.80	2.03	10.42
90	48.81	40.45	17.64	22.86	22.73	60.99	60.41	7.08	11.60
120	48.93	40.66	25.12	28.42	25.82	58.98	62.38	4.94	11.60

Calculation of chlorine conversion

Table 5. Conversion in the FGLP membrane

Time (min)	300 ppm					600 ppm		150 ppm	
	pH1	pH2	pH4	pH6	pH7	pH2	pH6	pH2	pH6
0	0.00	0.00	0.00	0.00	0.00	0.00	0.00	0.00	0.00
5	7.63	3.54	3.51	3.49	0.81	8.00	1.44	6.08	1.86
10	13.08	7.63	8.01	4.83	1.49	9.38	2.49	11.94	2.57
15	17.17	11.72	11.61	6.18	2.17	14.91	3.76	17.80	3.74
20	19.90	15.81	17.92	7.52	2.86	17.67	4.61	22.48	6.08
30	23.99	22.63	23.32	7.52	3.54	23.19	6.73	31.86	6.08
60	33.54	36.26	32.33	10.21	5.58	29.40	8.42	48.26	6.08
90	38.99	38.99	44.04	14.25	6.54	33.54	10.96	59.98	7.25
120	44.45	48.54	49.44	16.94	7.63	38.37	8.30	71.69	7.25

A.2. DATA TABLE FOR THE GVHP MEMBRANE

Calculation of chlorine concentration

Table 1. Chlorine concentration of GVHP membrane at 300ppm

Time (min)	pH1		pH2		pH4		PH6		pH7	
	C_{brine} (ppm)	C_{NaOH} (ppm)	C_{brine} (ppm)	C_{NaOH} (ppm)	C_{brine} (ppm)	C_{NaOH} (ppm)	C_{brine} (ppm)	C_{NaOH} (ppm)	C_{brine} (ppm)	C_{NaOH} (ppm)
0	300.23	0.00	301.93	0.00	303.64	0.00	300.23	0.00	298.54	0.00
5	241.57	16.60	280.85	12.52	299.40	0.28	296.04	2.32	290.21	0.28
10	187.10	45.17	213.41	32.93	290.92	6.40	291.85	6.40	281.88	8.44
15	153.58	61.50	188.12	49.25	286.68	12.52	287.66	8.44	269.38	8.44
20	111.68	69.66	171.26	69.66	273.96	20.69	275.09	16.60	261.05	12.52
30	82.35	81.90	141.76	102.31	265.48	24.77	266.71	16.60	256.89	16.60
60	23.69	106.39	78.53	126.80	257.00	26.81	258.33	24.77	246.48	20.69
90	15.31	114.55	44.81	147.20	240.04	39.05	249.95	26.81	246.48	22.73
120	6.93	122.72	32.17	159.45	231.56	47.21	241.57	27.22	242.31	26.81

Table 2. Chlorine concentration of GVHP membrane at 600ppm

Time (min)	pH2		PH6	
	C_{brine} (ppm)	C_{NaOH} (ppm)	C_{brine} (ppm)	C_{NaOH} (ppm)
0	601.91	0.00	618.67	0.00
5	455.26	53.34	610.29	4.36
10	346.32	77.82	601.91	8.44
15	279.28	106.39	593.53	16.60
20	191.29	126.80	585.15	16.60
30	136.82	155.37	568.39	24.77
60	44.64	196.18	564.20	37.01
90	15.31	204.34	551.63	45.17
120	3.46	208.42	534.87	57.42

able 3. Chlorine concentration of GVHP membrane at 150ppm

Time (min)	pH2		PH6	
	C_{brine} (ppm)	C_{NaOH} (ppm)	C_{brine} (ppm)	C_{NaOH} (ppm)
0	157.77	0	142.91	0
5	128.44	8.44	142.91	0.00
10	94.92	16.60	135.05	0.00
15	86.54	16.60	135.05	3.96
20	69.78	24.77	135.05	4.16
30	40.45	32.93	127.19	4.76
60	19.50	41.09	127.19	5.56
90	11.12	49.25	119.33	7.15
120	6.93	57.42	111.47	8.34

Calculation of chlorine losses

Table 4. Losses in the GVHP membrane

Time (min)	300 ppm					600 ppm		150 ppm	
	pH1	pH2	pH4	pH6	pH7	pH2	pH6	pH2	pH6
0	0.00	0.00	0.00	0.00	0.00	0.00	0.00	0.00	0.00
5	14.01	2.83	1.30	0.62	2.70	15.50	0.65	13.24	0.00
10	22.64	18.41	2.08	0.66	2.75	29.53	1.34	29.31	5.50
15	28.36	21.38	1.46	1.37	6.94	35.93	1.38	34.62	2.73
20	39.60	20.20	2.96	2.84	8.36	47.15	2.73	40.07	2.59
30	45.29	19.16	4.41	5.63	8.39	51.46	4.12	53.49	7.67
60	56.67	31.99	6.53	5.71	10.51	59.99	2.82	61.60	7.11
90	56.75	36.40	8.08	7.82	9.83	63.51	3.53	61.73	11.50
120	56.82	36.54	8.19	10.47	9.85	64.80	4.26	59.22	16.16

Calculation of chlorine conversion

Table 5. Conversion in the GVHP membrane

Time (min)	300 ppm					600 ppm		150 ppm	
	pH1	pH2	pH4	pH6	pH7	pH2	pH6	pH2	pH6
0	0.00	0.00	0.00	0.00	0.00	0.00	0.00	0.00	0.00
5	5.53	4.15	0.09	0.77	0.09	8.86	0.70	5.35	0.00
10	15.05	10.91	2.11	2.13	2.83	12.93	1.36	10.52	0.00
15	20.48	16.31	4.12	2.81	2.83	17.68	2.68	10.52	2.77
20	23.20	23.07	6.81	5.53	4.19	21.07	2.68	15.70	2.91
30	27.28	33.89	8.16	5.53	5.56	25.81	4.00	20.87	3.33
60	35.44	42.00	8.83	8.25	6.93	32.59	5.98	26.05	3.89
90	38.16	48.75	12.86	8.93	7.61	33.95	7.30	31.22	5.00
120	40.87	52.81	15.55	9.07	8.98	34.63	9.28	36.39	5.84